3 Some Methods for the Global Analysis of Dynamic Games Represented by Iterated Noninvertible Maps

Anna Agliari[1], Gian-Italo Bischi[2] and Laura Gardini[2]

[1]Istituto di Econometria e Matematica AEFA, Università Cattolica di Milano, Italy
[2]Istituto di Scienze Economiche, Università di Urbino, Italy

1 Introduction

The time evolution of an oligopoly system is often described as an n-players game which is played repeatedly, in the sense that at each discrete time period $t = 0, 1, ..., n$ producers choose their actions, $x_1(t), ..., x_n(t)$, by solving an optimization problem based on the knowledge of the actions observed in the past. For example, the classical Cournot adjustment (see Cournot, 1838, Teocharis, 1960, and many others) is obtained by assuming that at each period any player chooses its own production strategy which is a best response to the choices of the competitors in the previous period.

This is often expressed in the form of a discrete dynamical system defined in a given strategy space $S \subseteq R^n$. Given an initial condition $x(0) \in S$, the sequence of actions $x(t)$, $t \in N$, is obtained inductively by the iteration of a map $T : S \to S$ defined by

$$\mathbf{x}' = T(\mathbf{x}) \tag{1}$$

where $'$ denotes the unit-time advancement operator, that is, if the right hand side variables represent the actions at time period t then the left hand side represents the set of actions at time $(t + 1)$.

A dynamic process defined by the iterated map (1) may converge to a given steady state (or equilibrium) or to a more complex attractor. Indeed, as shown in a pioneering paper by Rand, 1978, quite complex dynamics, with periodic and chaotic trajectories, may characterize the long run behavior of duopoly games (see also Postom and Stewart, 1978). Examples of economically interesting discrete time dynamic oligopoly games, showing complex

dynamics, have been given by Dana and Montrucchio, 1986, Puu, 1991, 1997, 2000, Kopel, 1996, Agiza et al., 1999, Bischi et al., 2000a, 2001a, Agliari et al., 2000b, just to quote a few. In these papers it is shown that dynamic Cournot oligopoly games may have time evolutions which never settle to a steady state, and in the long run they exhibit bounded dynamics which may be periodic, or quasi-periodic or chaotic. In such cases, a delimitation of a bounded region of the strategy space where the system dynamics are ultimately trapped, despite of the complexity of the long-run time patterns, may be an useful information for practical applications. Moreover, as some parameters are varied, global bifurcations may cause sudden qualitative changes in the properties of the attracting sets (see the contact bifurcations in Mira et al., 1996 and the so called crises in Grebogi et al., 1983).

Another problem which often arises in the study of nonlinear maps which describe dynamic oligopoly games concerns the existence of several attracting sets, each with its own basin of attraction. In this case, a problem of equilibrium selection arises (see Van Huyck et al., 1994, Bischi and Kopel, 2001) because the dynamic process becomes path-dependent, i.e. which kind of long run dynamics is chosen depends on the starting condition of the game. This opens the question of the delimitation of the basins of attraction and their changes as the parameters of the model vary.

These two problems lead to two different routes to complexity, one related to the complexity of the attracting sets which characterize the long run time evolution of the dynamic process, the other one related to the complexity of the boundaries which separate the basins when several coexisting attractors are present. These two different kinds of complexity are not related in general, in the sense that very complex attractors may have simple basin boundaries, whereas boundaries which separate the basins of simple attractors, such as coexisting stable equilibria, may have very complex structures.

Both the questions outlined above require an analysis of the global dynamical properties of the dynamical system, that is, an analysis which is not based on the linear approximation of the map (1). When the map T is noninvertible (i.e. "many-to-one") the global dynamical properties can be usefully characterized by the method of critical sets, a powerful tool introduced in the seventies (see Gumovsky and Mira, 1980a,b and references therein, Mira et al. 1996, Abraham et al. 1997) but only recently employed in the study of dynamic modelling of economic and financial systems (see e.g. Gardini, 1992, Bischi et al., 1999b,c, 2000b, Agliari et al, 2000a, Puu 2000, Bischi and Kopel 2001, Bischi et al., 2001b, Dieci et al., 2001, Chiarella et al 2001a,b). Indeed, several dynamic models of oligopoly games are represented by the

iteration of a noninvertible map , i.e. a point transformation T which maps distinct points into the same point. Loosely speaking, this can be expressed by saying that the map "folds and pleats" the state space. As we shall describe in the following, the folding action associated with the application of a noninvertible map, as well as the "unfolding" associated with the geometric action of the inverses, can be described by using the formalism of critical sets. The repeated application of a noninvertible map repeatedly folds the state space along the critical sets and their images, and often this allows one to define a bounded region where asymptotic dynamics are trapped. Instead, the repeated application of the inverses "repeatedly unfolds" the state space, so that a neighborhood of an attractor may have preimages far from it. This may give rise to complicated topological structures of the basins, which may be formed by the union of non connected portions.

The paper is organized as follows. In section 2 we recall some definitions and properties of noninvertible maps. In section 3 we describe the construction of absorbing regions and in section 4 we recall the main contact bifurcations which lead to complex basins of attraction. In section 5 we describe the properties of a Cournot duopoly game and in section 6 we consider the special case of with symmetric duopoly games (i.e. duopoly games with identical players) leading to chaos synchronization problems and riddled basins.

2 Noninvertible maps: Basic definitions and properties

In this section we give some basic definitions and properties, and a minimal vocabulary, about the theory of noninvertible maps of the plane and the method of critical sets. A map $T : S \to S$, $S \subseteq R^n$, like the one defined in (1), transforms a point $x \in S$ into a unique point $x' \in S$. The point x' is called the rank-1 image of x, and a point x such that $T(x) = x'$ is a rank-1 preimage of x'. Starting from an initial condition $x_0 \in S$, the repeated application (iteration) of T uniquely defines a trajectory

$$\tau(\mathbf{x}_0) = \left\{\mathbf{x}(t) = T^t(\mathbf{x}_0), t = 0, 1, 2, ...\right\}, \tag{2}$$

where T^0 is the identity map and $T^t = T(T^{t-1})$.

A set $A \subset R^n$ is trapping if it is mapped into itself, $T(A) \subseteq A$, i.e. if $x \in A$ then $T(x) \in A$. A trapping set is invariant if it is mapped onto itself: $T(A) = A$, i.e. all the points of A are images of points of A. A closed invariant set A is an attractor if it is asymptotically stable, i.e. if a neighborhood U of A exists such that $T(U) \subseteq U$ and $T^t(x) \to A$ as

$t \to +\infty$ for each $x \in U$.

The Basin of an attractor A is the set of all points that generate trajectories converging to A

$$\mathcal{B}(A) = \left\{ \mathbf{x} | T^t(\mathbf{x}) \to A \quad \text{as } t \to +\infty \right\} \tag{3}$$

Starting from the definition of stability, let $U(A)$ be a neighborhood of an attractor A whose points converge to A. Of course $U(A) \subseteq B(A)$, but also the points of the phase space which are mapped inside U after a finite number of iterations belong to $B(A)$. Hence, the total basin of A (or briefly the basin of A) is given by

$$\mathcal{B}(A) = \bigcup_{n=0}^{\infty} T^{-n}(U(A)) \tag{4}$$

where $T^{-1}(x)$ represents the set of the rank-1 preimages of x (i.e. the points mapped into x by T), and $T^{-n}(x)$ represents the set of the rank-n preimages of x (i.e. the points mapped into x after n applications of T).

If $x \neq y$ implies $T(x) \neq T(\mathbf{y})$ then T is an invertible map, because the inverse mapping that gives $x = T^{-1}(\mathbf{x}')$ is uniquely defined; otherwise T is a noninvertible map. So, noninvertible means "many-to-one", that is, distinct points $x \neq y$ may have the same image, $T(x) = T(\mathbf{y}) = x'$. Hence, several rank-1 preimages may exist and the inverse relation $x = T^{-1}(\mathbf{x}')$ may be multivalued. Geometrically, the action of a noninvertible map T can be expressed by saying that it "folds and pleats" the plane, so that the two distinct points p_1 and p_2 are mapped into the same point p. This is equivalently stated by saying that several inverses are defined in p, and these inverses "unfold" the plane.

For a noninvertible map (1) R^n can be subdivided into regions Z_k, $k \geq 0$, whose points have k distinct rank-1 preimages. Generally, as the point x' varies in R^n, pairs of preimages appear or disappear as this point crosses the boundaries separating different regions. Hence, such boundaries are characterized by the presence of at least two coincident (merging) preimages. This leads to the definition of the critical sets, one of the distinguishing features of noninvertible maps (Gumovski and Mira, 1980, Mira et al., 1996):

Definition. The critical set CS of a continuous map T is defined as the locus of points having at least two coincident $rank - 1$ preimages, located on a set CS_{-1} called set of merging preimages.

The critical set CS is the n-dimensional generalization of the notion of critical value (when it is a local minimum or maximum value) of a one-dimensional map[1], and of the notion of critical curve LC (from the French "Ligne Critique", following Gumowski and Mira, 1980), of a noninvertible two-dimensional map. The set CS_{-1} is the generalization of the notion of critical point (when it is a local extremum point) of a one-dimensional map, and of the fold curve LC_{-1} of a two-dimensional noninvertible map. The critical set CS is generally formed by $(n-1)$-dimensional hypersurfaces of R^n, and portions of CS separate regions Z_k of the phase space characterized by a different number of $rank-1$ preimages, for example Z_k and Z_{k+2} (this is the standard occurrence).

From the definition given above it is clear that the relation $CS = T(CS_{-1})$ holds, and the points of CS_{-1} in which the map is continuously differentiable are necessarily points where the Jacobian determinant vanishes, so that if T is smooth we have :

$$CS_{-1} \subseteq J_0 = \{p \in \mathbb{R}^n | \det DT(p) = 0\} \tag{5}$$

In fact, in any neighborhood of a point of CS_{-1} there are at least two distinct points which are mapped by T in the same point. Accordingly, the map is not locally invertible in points of CS_{-1}.

In order to explain the geometric meaning of the critical sets, let us consider a portion of CS, say $\widehat{CS}$, which separates two regions Z_k and Z_{k+2} of the phase space, and let $\widehat{CS}_{-1}$ be the corresponding locus of merging preimages, i.e. $\widehat{CS} = T\left(\widehat{CS}_{-1}\right)$. This means that two inverses of T exist, say T_1^{-1} and T_2^{-1}, which are defined in the region Z_{k+2} (and have respective ranges in the regions R_1 and R_2 separated by $\widehat{CS}_{-1}$). Both inverses merge on $\widehat{CS}_{-1}$ (i.e. they give merging preimages on $\widehat{CS}_{-1}$) and no longer exist in the region Z_k. Now, let $U \subset R^n$ be a ball which intersects $\widehat{CS}_{-1}$ in $D = U \cap \widehat{CS}_{-1}$. Then $T(D) \subseteq \widehat{CS}$, and $T(U)$ is "folded" along $\widehat{CS}$ into the region Z_{k+2}. In fact, considering the two portions of U separated by $\widehat{CS}_{-1}$, say $U_1 \in R_1$ and $U_2 \in R_2$, we have that $T(U_1) \cap T(U_2)$ is a non-empty set included in the region Z_{k+2}, which is the region whose points p' have rank-1 preimages $p_1 = T_1^{-1}(p') \in U_1$ and $p_2 = T_2^{-1}(p') \in U_2$. This means that two points $p_1 \in U_1$ and $p_2 \in U_2$, located at opposite sides with respect to $\widehat{CS}_{-1}$, are mapped in the same side with respect to $\widehat{CS}$, in the

[1]This terminology, and notation, originates from the notion of critical points as it is used in the classical works of Julia and Fatou.

region Z_{k+2}. This is also expressed by saying that the ball U is "folded" by T along CS on the side with more preimages (examples in two dimensions are given below, see e.g. Fig. 7). The same concept can be equivalently expressed by stressing the "unfolding" action of T^{-1}, obtained by the application of the two distinct inverses in Z_{k+2} which merge along CS, because if we consider a ball $V \subset Z_{k+2}$, then the set of its $rank-1$ preimages $T_1^{-1}(V)$ and $T_2^{-1}(V)$ is made up of two balls $T_1^{-1}(V) \in R_1$ and $T_2^{-1}(V) \in R_2$, and these balls are disjoint if $V \cap \widehat{CS} = \emptyset$.

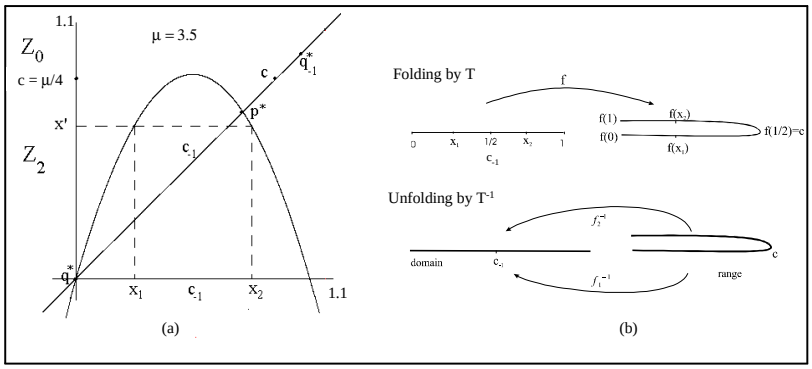

Figure 1: (a) The logistic map (b) Folding and unfolding actions.

For one-dimensional continuous maps $x' = f(x)$, $x \in R$, the critical set is formed by the local maximum or minimum values. For example, the well known logistic map (Fig.1a)

$$x' = f(x) = \mu x(1-x) \tag{6}$$

has a unique critical point $c = \mu/4$, which separates the real line into the two subsets: $Z_0 = (c, +\infty)$, where no inverses are defined, and $Z_2 = (-\infty, c)$, whose points have two rank-1 preimages, computed by the two inverses

$$x_1 = f_1^{-1}(x') = \frac{1}{2} - \frac{\sqrt{\mu\,(\mu - 4x')}}{2\mu}; \quad x_2 = f_2^{-1}(x') = \frac{1}{2} + \frac{\sqrt{\mu\,(\mu - 4x')}}{2\mu} \tag{7}$$

If $x' \in Z_2$, its two rank-1 preimages, computed according to (7), are located symmetrically with respect to the point $c_{-1} = 1/2 = f_1^{-1}(\mu/4) = f_2^{-1}(\mu/4)$, i.e. c_{-1} is the point where the two merging preimages of c are

located. Of course, since the map (6) is differentiable, at c_{-1} the first derivative vanishes. However, we remark that in general the condition of vanishing derivative is not sufficient to define c_{-1}, because such condition may also be satisfied by points which are not local extrema (e.g. the inflection points with horizontal tangent). Moreover, a critical point may even be a point where the map is not differentiable, as it happens for continuous piecewise differentiable maps where critical points are located at the kinks where local maxima and minima are formed in the points at which two branches having slopes of opposite sign join, such as the well known tent map or other piecewise linear maps (see Fig.2a).

The importance of the critical points lies in the fact that they separate regions Z_k characterized by different number of preimages. We note however that this property is not a characteristic only of the critical points, because the boundary of a region Z_k may also be a particular set, called prefocal set, whose properties are associated with inverses not defined in the whole space, as shown in Bischi et al. 1999a.

In order to explain the action of a critical point, let us consider again the logistic map and let us notice that, as x moves from 0 to 1, the corresponding image $f(x)$ spans the interval $[0, c]$ twice, the critical point c being the turning point. In other words, if we consider how the segment $\gamma = [0, 1]$ is transformed by the map f we can say that it is folded and pleated to obtain the image $\gamma' = [0, c]$. This folding gives a geometric reason why two distinct points of γ, say x_1 and x_2, located symmetrically with respect to the point $c_{-1} = 1/2$, are mapped into the same point $x' \in \gamma'$ due to the folding action of f (Fig.1b). This is a geometric interpretation of the fact that (6) is a two-to-one map.

The same arguments can be explained by looking at the two inverse mappings f_1^{-1} and f_2^{-1} defined in $(-\infty, \mu/4]$ according to (7). We can consider the range of the map f formed by the superposition of two half-lines $(-\infty, \mu/4]$, joined at the critical point $c = \mu/4$ (Fig.1b), and on each of these half-lines a different inverse is defined. With other words, instead of saying that two distinct maps are defined on the same half-line we say that the range is formed by two distinct half lines on each of which a unique inverse map is defined. This point of view gives a geometric visualization of the definition of the critical point c of rank-1 as the point in which two distinct inverses merge. The action of the multivalued inverse, say $f^{-1} = f_1^{-1} \cup f_2^{-1}$, causes an unfolding of the range by mapping c into c_{-1} and by opening the two half-lines one on the right and one on the left of c_{-1}, so that the whole real line R is covered. Of course, a small segment γ' inside Z_2

and not including c, is splitted by the two inverses into two disjoint segments, located at opposite sides with respect to c_{-1}.

Up to now we have considered continuous maps, but the properties of critical points can easily be extended also to a discontinuous map T. In this case a point of discontinuity may be a critical point of T. This happens when the ranges of the map on the two sides of the discontinuity have an overlapping zone, so that at least one of the two limiting values of the function at the discontinuity separates regions having a different number of rank-1 preimages. The difference with respect to the continuous case is that now the number of distinct rank-1 preimages through a critical point differs generally by one (instead of two), that is, a critical value c (in general the critical set CS) separates regions Z_k and Z_{k+1}. An example is shown in Fig.2b, with a one-dimensional map. The discontinuity point is a critical point c_{-1}, and both the two limiting values of the function in c_{-1} are critical points, say c_a and c_b, associated with c_{-1}, as both c_a and c_b separate regions Z_1 and Z_2. Notice that now the critical points have no merging rank-1 preimages. Consider for example the critical point c_b in Fig.2b. The two distinct rank-1 preimages of c_b are the critical point c_{-1} and the so called "excess rank-1 preimage" $c^e_{-1,b}$. More on the properties and bifurcations of discontinuous maps of the plane can be found in Mira et al., 1996. In the following sections we shall only consider, for the sake of simplicity, continuous maps.

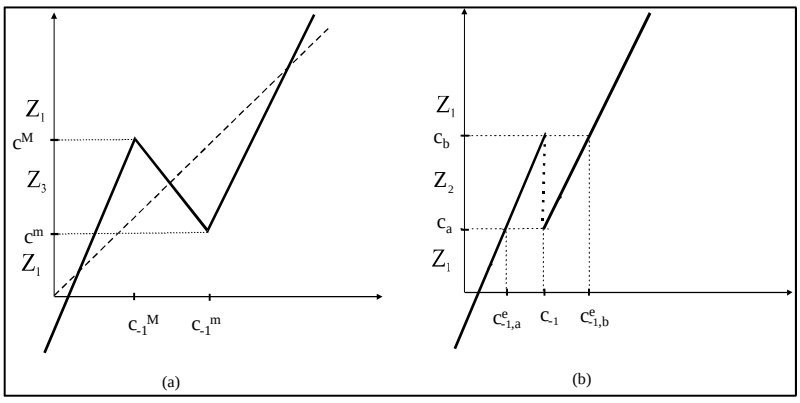

Figure 2: (a) A piecewise linear noninvertible map. (b) A discontinuous noninvertible map.

Another interpretation of the folding action of the unimodal map f is

the following. Since $f(x)$ is increasing for $x \in [0, 1/2)$ and decreasing for $x \in (1/2, 1]$, then its application to a segment $\gamma_1 \subset [0, 1/2)$ is orientation preserving, whereas its application to a segment $\gamma_2 \subset (1/2, 1]$ is orientation reversing. This suggests that an application of f to a segment $\gamma_3 = [a, b]$ including the point $c_{-1} = 1/2$ preserves the orientation of the portion $[a, c_{-1}]$, i.e. $f([a, c_{-1}]) = [f(a), c]$, whereas it reverses the portion $[c_{-1}, b]$, i.e. $f([c_{-1}, b]) = [f(b), c]$, so that $\gamma_3' = f(\gamma_3)$ is folded, the folding point being the critical point of rank-1 c.

The extension of these concepts to the case of two-dimensional noninvertible maps leads us to the notion of critical curves. We present here some geometric characterizations of the action of the critical curves, because they present some new features with respect to the one dimensional case, and their properties can often be used as a useful visualization for the analogous properties of n-dimensional cases, with $n > 2$. Moreover, dynamic duopoly games, represented by a continuous map of the plane into itself $T : (x_1(t), x_2(t)) \to (x_1(t+1), x_2(t+1))$ defined as

$$T : \begin{cases} x_1' = T_1(x_1, x_2) \\ x_2' = T_2(x_1, x_2) \end{cases}, \tag{8}$$

constitute the simplest oligopolies, and are often studied in the literature.

If we solve the system of the two equations (8) with respect to the unknowns x_1 and x_2, then, for a given (x_1', x_2'), we may have several solutions, representing rank-1 preimages (or backward iterates) of (x_1', x_2'), say $(x_1, x_2) = T^{-1}(x_1', x_2')$, where T^{-1} is in general a multivalued relation. In this case we say that T is noninvertible, and the critical curves LC are the boundaries which separate regions of the plane characterized by a different number of rank-1 preimages. Along LC at least two inverses give merging preimages, located on the set denoted by LC_{-1}. For a continuous and (at least piecewise) differentiable noninvertible map of the plane, the study of the sign of the Jacobian determinant can help one to find the critical curves, because the set LC_{-1} is included in the set where $\det DT(x_1, x_2)$ changes sign, since T is locally an orientation preserving map near points (x_1, x_2) such that $\det DT(x_1, x_2) > 0$ and orientation reversing if $\det DT(x_1, x_2) < 0$, and $LC = T(LC_{-1})$.

In order to understand this point, let us recall that when a linear transformation $x' = Ax$ of the plane onto itself

$$G : \begin{cases} x_1' = a_{11}x_1 + a_{12}x_2 \\ x_2' = a_{21}x_1 + a_{22}x_2 \end{cases} \tag{9}$$

is applied to a plane figure F, then the area of the transformed figure $F' = G(F)$ grows, or shrinks, by a factor $\rho = |\det A|$ with respect to the area of F, being A the Jacobian matrix DG, and if $\det A > 0$ then the orientation of the figure on which (9) is applied is preserved, whereas if $\det A < 0$ then the orientation is reversed. This property of a linear two-dimensional map can be applied to the linear approximation of (8) in a neighborhood of a point $p = (x_1, x_2)$, given by an affine map, the Jacobian matrix DT evaluated at the point p:

$$\mathbf{DT}(\mathbf{p}) = \begin{bmatrix} \partial T_1/\partial x_1 & \partial T_1/\partial x_2 \\ \partial T_2/\partial x_1 & \partial T_2/\partial x_2 \end{bmatrix} \tag{10}$$

In fact, a small area around a point $p = (x_1, x_2)$ is reduced (or expanded) by a factor $\rho(x_1, x_2) = |\det DT(x_1, x_2)|$, and if in a neighborhood of p the Jacobian determinant is positive (negative), then the map (8) is locally orientation preserving (reversing). This gives an intuitive visualization of the relation between the locus of points where the Jacobian determinant changes sign and the folding properties of continuous two-dimensional noninvertible maps (see Fig.3).

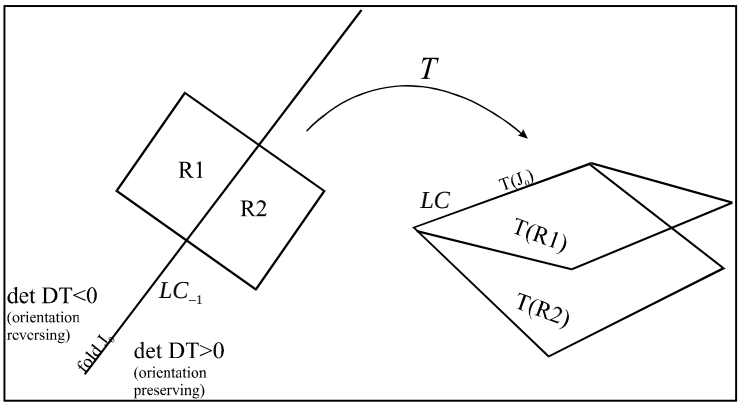

Figure 3: Folding properties of a continuous two-dimensional map.

This implies that if the map (8) is continuously differentiable in the whole plane, then

$$LC_{-1} \subseteq J_0 = \left\{(x_1, x_2) \in \mathbb{R}^2 | \det DT(x_1, x_2) = 0\right\} \tag{11}$$

Let us remark, however, that condition of vanishing Jacobian is necessary

for differentiable maps, but not sufficient to detect a critical point of LC_{-1} as defined above (i.e. the inclusion in (11) may be strict).

In order to give a geometrical interpretation of the action of the multi-valued inverse relation T^{-1}, it is useful to consider a region Z_k as the superposition of k sheets, each one associated with a different inverse. Such a representation is known as Riemann foliation of the plane (see e.g. Mira et al., 1996). Different sheets are connected by folds joining two sheets, and the critical curve LC belongs to the projections of such folds on the phase plane (note however that the vice-versa is not necessarily true, due to the properties associated with prefocal sets, see Bischi et al., 1999a).

We illustrate these concepts by some examples. Let us consider the quadratic map (see Mira et al., 1996, Abraham et al., 1997) defined by

$$T : \begin{cases} x' = ax + y \\ y' = b + x^2 \end{cases} \tag{12}$$

This is a noninvertible map. In fact, given x' and y', if we try to solve the algebraic system with respect to the unknowns x and y we get two solutions, given by

$$T_1^{-1} : \begin{cases} x = -\sqrt{y' - b} \\ y = x' + a\sqrt{y' - b} \end{cases} \quad ; \qquad T_2^{-1} : \begin{cases} x = \sqrt{y' - b} \\ y = x' - a\sqrt{y' - b} \end{cases} \tag{13}$$

if $y' \geq b$, and no solutions if $y' < b$. In other words, (12) is a $Z_0 - Z_2$ noninvertible map, where Z_0 (region whose points have no preimages) is the half plane $Z_0 = \{(x, y) \,|\, y < b\}$ and Z_2 (region whose points have two distinct rank-1 preimages) is the half plane $Z_2 = \{(x, y) \,|\, y > b\}$. The line $y = b$, which separates these two regions, is the locus of points having two merging rank-1 preimages, located on the line $x = 0$. Hence the line $y = b$ is LC and the line $x = 0$ is LC_{-1} (see Fig.4.). Being (12) a continuously differentiable map, the points of LC_{-1} necessarily belong to the set of points at which the Jacobian determinant vanishes, i.e. $LC_{-1} \subseteq J_0$, where

$$J_0 = \{(x, y) \,|\, \det DT(x, y) = 0\}$$

and, since for the map (12) we have

$$\det\left(DT(x, y)\right) = \det\left(\begin{bmatrix} a & 1 \\ 2x & 0 \end{bmatrix}\right) = -2x$$

in this case LC_{-1} coincides with J_0 (the y axis $x = 0$). The critical curve LC is the image by T of LC_{-1}

$$LC = T(LC_{-1}) = T\left(\{x = 0\}\right) = \{(x, y) \,|\, y = b\}$$

We can consider the region Z_2 of the two-dimensional noninvertible map (12) as formed by the superposition of two sheets, and on each of these sheets a different inverse map is defined. The two sheets join along the critical line LC, where the two inverses merge (see Fig.4). This is the Riemann foliation for the $Z_0 - Z_2$ map (12). The action of the inverses, $T^{-1} = T_1^{-1} \cup T_2^{-1}$, causes an unfolding of the sheets by opening these sheets at opposite sides with respect to the line LC_{-1}. That is, given a point $(x', y') \in Z_2$ the preimages $T_1^{-1}(x', y')$ and $T_2^{-1}(x', y')$ are located on the right and on the left of LC_{-1} respectively.

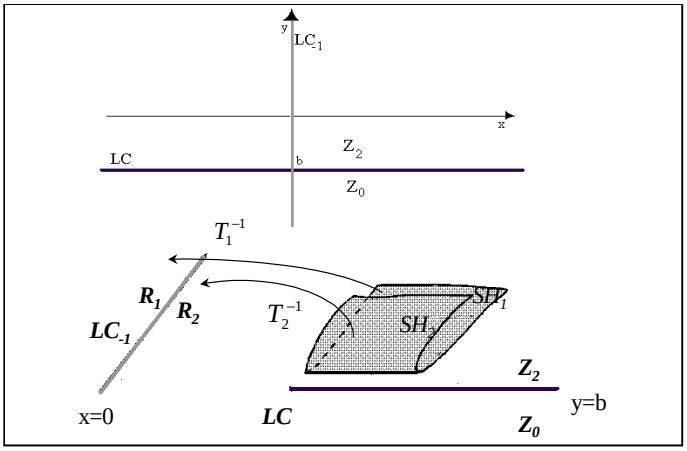

Figure 4: Riemann foliation associated with the map T in (12).

We propose another example, given by the map $T : (x, y) \to (x', y')$ defined by

$$T : \begin{cases} x' = \mu_1 y(1-y) + \varepsilon_1(y-x) \\ y' = \mu_2 x(1-x) + \varepsilon_2(x-y) \end{cases} \tag{14}$$

This is a $Z_0 - Z_2 - Z_4$ noninvertible map. In fact, given x' and y', if we solve the fourth degree algebraic system with respect to the unknowns x and y we may get four, two or no real solutions. The inverse maps are not easy to write by an elementary analytic form, since they are obtained by solving a fourth degree algebraic system. Nevertheless, it is easy to draw critical curves in order to obtain the boundaries separating the regions Z_k characterized by

different numbers of inverses. In fact, from the Jacobian matrix

$$DT(x,y) = \begin{bmatrix} -\varepsilon_1 & \mu_1(1-2y)+\varepsilon_1 \\ \mu_2(1-2x)+\varepsilon_2 & -\varepsilon_2 \end{bmatrix}$$

the equation of LC_{-1}, defined by $\det DT(x,y) = 0$, is given by

$$4\mu_1\mu_2 xy - 2\mu_2(\mu_1+\varepsilon_1)x - 2\mu_1(\mu_2+\varepsilon_2)y + \mu_1\mu_2 + \mu_1\varepsilon_2 + \mu_2\varepsilon_1 = 0.$$

Hence LC_{-1} is formed by the two branches, say $LC_{-1}^{(a)}$ and $LC_{-1}^{(b)}$, of an equilateral hyperbola (see Fig.5a). Also the critical set of rank-1 $LC =$

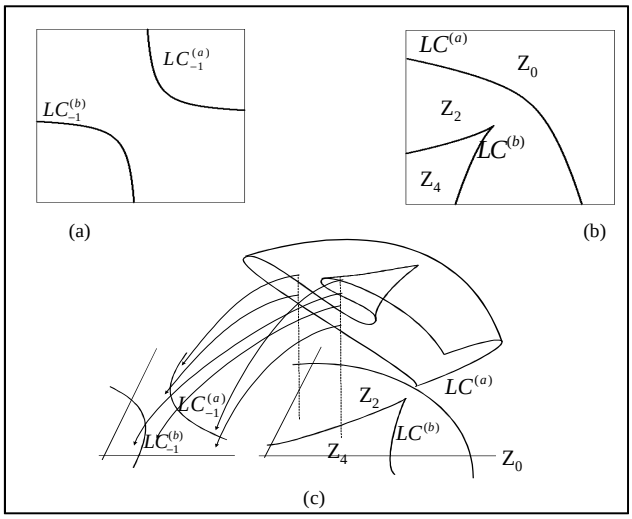

Figure 5: (a) LC_{-1}. (b) LC and the Zones $Z_2 - Z_4 - Z_0$. (c) Riemann foliation for the map (14).

$T(LC_{-1})$, obtained by taking the image by T of LC_{-1}, is formed by two disjoint branches: $LC = LC^{(a)} \cup LC^{(b)}$, where $LC^{(a)} = T(LC_{-1}^{(a)})$ and $LC^{(b)} = T(LC_{-1}^{(b)})$ (see Fig.5b). The branch $LC^{(a)}$ separates the regions Z_0 and Z_2, the branch $LC^{(b)}$ separates the regions Z_2 and Z_4. The Riemann foliation associated with the map (14) is qualitatively sket-ched in Fig.5c. Notice that the cusp point of $LC^{(b)}$ is characterized by three merging preimages at the junction of two folds.

An important property of the critical curves is that when an arc γ crosses LC_{-1} then its image $T(\gamma)$ is folded along LC, so that it is entirely included

in the region characterized by an higher number of preimages. A qualitative picture is shown in Fig.6. The effect on a plane figure is shown in Fig.7, where the map (12) is applied to a circle crossing through LC_{-1}.

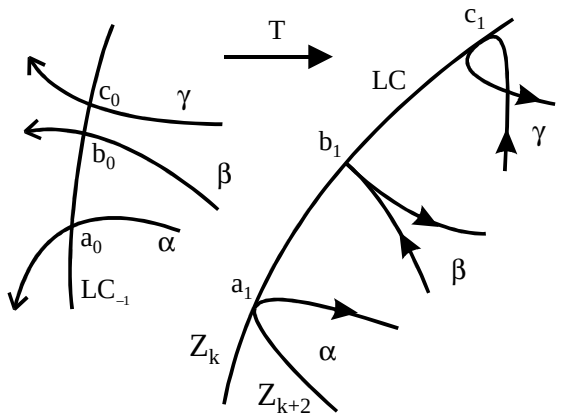

Figure 6: Folding of arcs crossing through LC_{-1}.

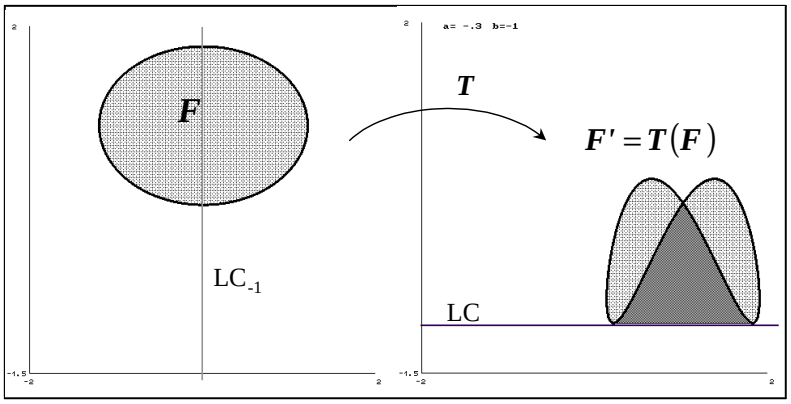

Figure 7: Folding of a circle crossing through LC_{-1}.

3 Absorbing regions, chaotic attractors and their delimitation.

Portions of the critical set CS and its images $CS_k = T^k(CS)$ can be used to obtain the boundaries of trapping regions where the asymptotic dynamics of the iterated points of a noninvertible map are confined. This can be easily explained for a one-dimensional noninvertible map, for example the quadratic map (6). In fact, it is quite evident that if we iterate the logistic map for $2 < \mu < 4$ starting from an initial condition inside the interval $[c_1, c]$, with $c_1 = f(c)$, no images can be obtained out of this interval (see Fig.8), i.e. the interval formed by the critical point c and its rank-1 image c_1 is trapping. Moreover, any trajectory generated from an initial condition in

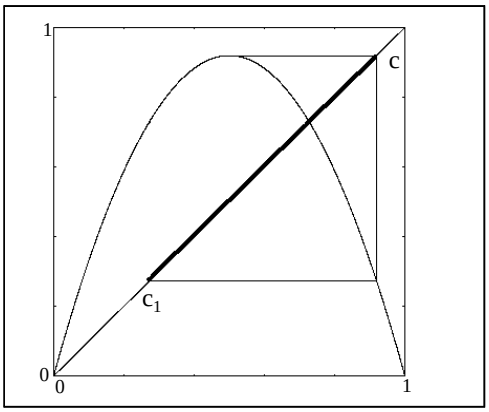

Figure 8: Absorbing interval

$(0, 1)$, enters $[c_1, c]$ after a finite number of iterations. Following the terminology introduced in Mira et al., 1996, the interval $[c_1, c]$ is called absorbing. In general, for an n-dimensional map, an absorbing region A (intervals in R, areas in R^2, volumes in R^3, ...) is defined as a bounded set whose boundary is given by portions of the critical set CS and its images of increasing order $CS_k = T^k(CS)$, such that a neighborhood $U \supset A$ exists whose point enter A after a finite number of iterations and then never escape it, since $T(A) \subseteq A$, i.e. A is trapping (see e.g. Mira et al., 1996 for more details). Loosely speaking, we can say that the iterated application of a noninvertible map, folding and folding again the space, defines trapping regions bounded by critical sets of increasing order.

Sometimes, smaller absorbing regions are nested inside a bigger one.

This can be illustrated, again, for the logistic map (6), as shown in Fig.9a, where inside the absorbing interval $[c_1, c]$ a trapping subset is obtained by higher rank images of the critical point, given by $A = [c_1, c_3] \cup [c_2, c]$. In Fig.9b it is shown that, for the same parameter value $\mu = 3.61$ as in Fig.9a, the iteration of the logistic map gives points which never escape A.

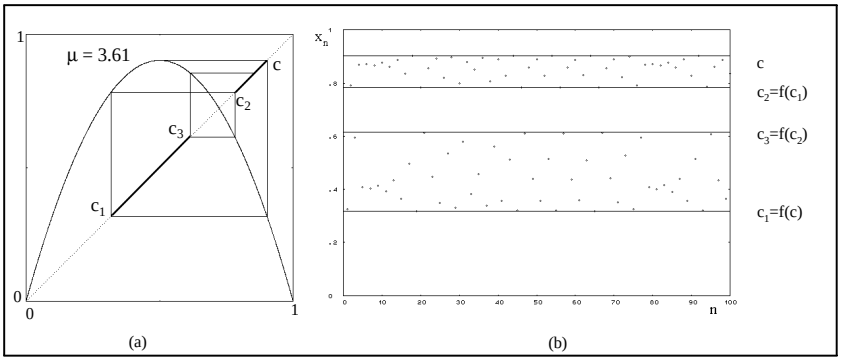

Figure 9: Absorbing intervals nested inside $[c_1, c]$.

An absorbing region A, for which the property $T(A) \subseteq A$ holds, may be invariant, i.e. exactly mapped into itself, $T(A) = A$, or strictly mapped into itself, $T(A) \subset A$. Moreover, several invariant absorbing regions may exist, one embedded into the other. In these cases the concept of minimal invariant absorbing region is often useful, where minimal means the smallest one, in the sense that no other smaller absorbing regions are nested inside it.

Inside an absorbing region one or more attractors may exist. However, if a chaotic attractor exists which fills up the absorbing region then it is also called chaotic region, and the boundary of the chaotic attractor is formed by portions of critical sets. This is the situation shown in Fig.9, where the absorbing interval $A = [c_1, c_3] \cup [c_2, c]$ is invariant and filled up by a chaotic trajectory, as shown in Fig.9b. To better illustrate this point, we also give a two-dimensional example, obtained by using the map (12). In Fig.10a a chaotic trajectory is shown, and in Fig.10b an absorbing area around it is obtained by the union of a segment of LC and three iterates $LC_i = T^i(LC)$, $i = 1, 2, 3$.

Indeed, following Mira et al., 1996, a practical procedure can be outlined in order to obtain the boundary of an absorbing area (although it is difficult to give a general method). Starting from a portion of LC_{-1}, approximately

taken in the region occupied by the area of interest, its images by T of increasing rank are computed until a closed region is obtained. When such a region is mapped into itself, then it is an absorbing area A. The length of the initial segment is to be taken, in general, by a trial and error method, although several suggestions are given in the books referenced above. Once an absorbing area A is found, in order to see if it is invariant or not the same procedure must be repeated by taking only the portion

$$\gamma = \mathcal{A} \cap LC_{-1} \tag{15}$$

as the starting segment. Then one of the following two cases occurs:

(case I) the union of m iterates of γ (for a suitable m) covers the whole boundary of A; in which case A is an invariant absorbing area, and

$$\partial\mathcal{A} \subset \bigcup_{k=1}^{m} T^k(\gamma) \tag{16}$$

(case II) no natural m exists such that $\bigcup_{i=1}^{m} T^i(\gamma)$ covers the whole boundary of A; in which case A is not invariant but strictly mapped into itself. An invariant absorbing area is obtained by $\cap_{n>0} T^n(A)$ (and may be obtained by a finite number of images of A).

The application of this procedure to the problem of the delimitation of the chaotic area of Fig.10 by portions of critical curves suggests us, on the basis of Fig.10b, to take a smaller segment γ and to take an higher number of iterates in order to obtain also the inner boundary. The result is shown in Fig.11. By five iterates we get the outer boundary, shown in Fig.11a, by more iterates also the inner boundary of the chaotic area is get, as shown in Fig.11b. As it can be clearly seen, and as clearly expressed by the strict inclusion in (16), the union of the images also include several arcs internal to the invariant area A. Indeed, the images of the critical arcs which are mapped inside the area play a particular role, because these curves represent the "foldings" of the plane under forward iterations of the map, and this is the reason why these inner curves often denote the portions of the region which are more frequently visited by a generic trajectory inside it (compare Fig.10a and Fig.11b); many examples are given in the literature on noninvertible maps, see e.g. Mira et al., 1996. The points close to a critical arc LC_i, $i \geq 0$, are more frequently visited because there are several distinct parts of the invariant area which are mapped in the same region (close to LC_i) in $i+1$ iterations.

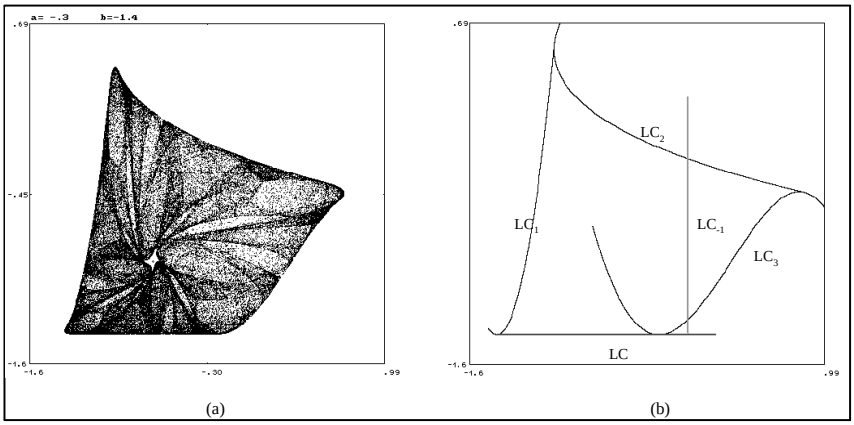

Figure 10: (a) Chaotic trajectory for a two-dimensional map. (b) The outer boundary of the chaotic area obtained by the segments of LC_k, $k = 1, 2, 3$.

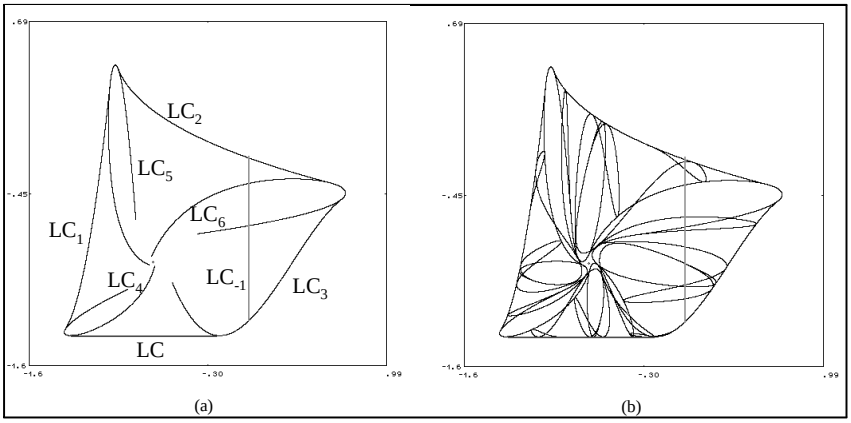

Figure 11: (a) Five iterates of LC give the outer boundary of the chaotic area shown in of Fig.10. (b) More iterates also give the inner boundary.

4. Contact bifurcations and the creation of complex basins

From (4) it is clear that the properties of the inverses are important in order to understand the structure of the basins and the main bifurcations which change their qualitative properties. In the case of noninvertible maps, the multiplicity of preimages may lead to basins with complex structures, such as multiply connected or non connected sets, sometimes formed by infinitely many non connected portions (see Mira et al., 1994, Mira and Rauzy, 1995, Mira et al., 1996, ch.5, Abraham et al., 1997,ch.5). In the context of noninvertible maps it is useful to define the immediate basin $B_0(A)$, of an attracting set A, as the widest connected component of the basin which contains A. Then the total basin can be expressed as

$$\mathcal{B}(A) = \bigcup_{n=0}^{\infty} T^{-n}(\mathcal{B}_0(A))$$

where $T^{-n}(x)$ represents the set of all the rank-n preimages of x, i.e. the set of points which are mapped in x after n iterations of the map T. The backward iteration of a noninvertible map repeatedly unfolds the phase space, and this implies that the basins may be non-connected, i.e. formed by several disjoint portions.

Also in this case, we first illustrate this property by using a one-dimensional map[2] In Fig.12 the graph of a $Z_1 - Z_3 - Z_1$ noninvertible map is shown, where two stable fixed points exist, denoted by O and p, whose basins $B(O)$ and $B(p)$ are represented along the diagonal by light and dark grey thick lines respectively. In Fig.12a the two basins are connected sets, bounded by the unstable fixed points q and r. As a parameter is varied, the critical point c (the local minimum), which separates the lower region Z_1 from the region Z_3, moves downwards, until it has a contact with the basin boundary q, and a crossing occurs if the parameter is further changed. Before the contact $c > q$ (see the enlargement in Fig.12b), whereas after the contact we have $c < q$. This implies that a portion of $B(O)$ enters Z_3, i.e. the segment $[c, q) = H_0$, thus causing the appearance of non connected portions of $B(O)$ nested inside $B(p)$. Indeed, infinitely many non connected portions (or holes) are suddenly created at the contact bifurcation, given by the preimages of any rank of the portion H_0 of $B(O)$ included into Z_3, see $H_{-i} = T^{-i}(H_0)$, $i = 1, 2, ...$, in Fig.12c. Before the bifurcation $B(p) = (q, r)$ (Fig.12a), after the bifurcation the basin of p is given

[2]The example is taken from an evolutionary game proposed in Bischi et al., 2001b.

by the immediate basin $B_0(p) = (q, q_{-1,1})$ (Fig.12c), and all its preimages, $B(p) = \bigcup_{n=0}^{\infty} T^{-n}(B_0)$, given by infinitely many segments that have the unstable fixed point r as limit point. So, the contact between the critical point c and the basin boundary q marks the transition from simple connected to non connected basins.

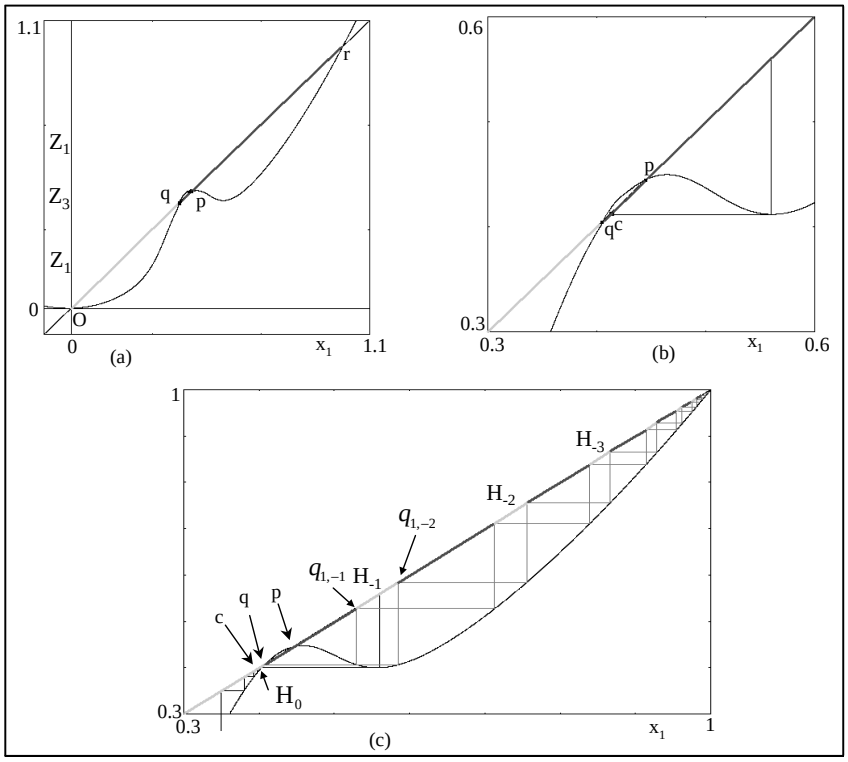

Figure 12: (a) Graph of a $Z_1 - Z_3 - Z_1$ noninvertible map and basins of attraction of p and O, before the contact between the critical point c and the basin boundary q. (b) Enlargement. (c) The basins of p and O after the contact.

Similar global bifurcations, due to contacts between critical sets and basin boundaries, also occur in higher dimensional maps. In general, the origin of complex topological structures of the basins, like those formed by non connected sets, can be easily explained on the basis of the geometrical properties of a noninvertible map. In fact, suppose that p is a fixed point of

T, i.e. $T(p) = p$. Hence one of the preimages of p is p itself, but if T^{-1} is multivalued in p, i.e. $p \in Z_k$, with $k \geq 2$, then other preimages of the fixed point p exist. If the fixed point is stable, and $B_0(p)$ is its immediate basin, then the total basin of p must also include all the rank-1 preimages of the points of $B_0(p)$, which may be also far (i.e. disjoint) from $B_0(p)$. Whenever such disjoint preimages belong to regions where many inverses exist, higher rank preimages of $B_0(p)$ must be included in the basin of p and so on[3]. Such behavior of the multivalued inverse of T may be better visualized by using the concept of Riemann foliation (see Fig.13).

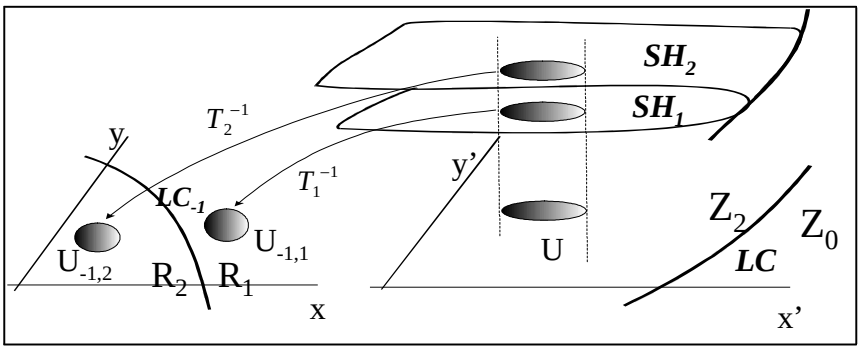

Figure 13: Riemann foliation which visualizes the basic mechanism for the creation of disconnected basins

Also in higher dimensional cases, the global bifurcations which give rise to complex topological structures of the basins, like those formed by non connected sets, can be explained in terms of contacts of basins boundaries and critical sets. In fact, if a parameter variation causes a crossing between a basin boundary and a critical set which separates different regions Z_k so that a portion of a basin enters a region where an higher number of inverses is defined, then new components of the basin may suddenly appear at the contact. However, for maps of dimension greater than 1, such kinds of bifurcations can be very rarely studied by analytical methods, since the analytical equations of such singularities are not known in general. Hence these studies are mainly performed by geometric and numerical methods.

[3]A similar reasoning applies to any kind of attractor, such as a periodic orbit (a cycle) or a chaotic set.

4.1 Basin bifurcations in a duopoly game with two stable Nash equilibria

We consider a Cournot duopoly game proposed in Kopel, 1996, for which the structure of the basins and their qualitative changes are analyzed in Bischi et al., 1999b. This game describes a market where, at each time period t, two firms decide their productions for the next period on the basis of best reply functions expressed as $q_i(t+1) = r_i(q_j(t))$, $i, j = 1, 2$, $i \neq j$, where the reaction functions r_i assume the form of logistic maps $r_i(q_j) = \mu_i q_j (1 - q_j)$ (in Kopel, 1996, these functions are derived as Best Responses). The dynamic duopoly game is obtained by assuming that competitors do not immediately adjust to the optimal quantity they computed on the basis of the profit maximization problem, but that they exhibit some kind of inertia: they only adjust their previous production quantities in the direction of the Best Response. The time evolution of the game is obtained by the iteration of the two-dimensional map $T : (q_1, q_2) \to (q_1', q_2')$ defined by

$$T : \begin{cases} q_1' = (1 - \lambda_1) q_1 + \lambda_1 \mu_1 q_2 (1 - q_2) \\ q_2' = (1 - \lambda_2) q_2 + \lambda_2 \mu_2 q_1 (1 - q_1) \end{cases} . \tag{17}$$

where the parameters $\lambda_i \in [0, 1]$, $i = 1, 2$, represent the speeds of adjustment. The fixed points of map (17), located at the intersections of the two reaction curves, coincide with the Nash equilibria of the duopoly game (see Kopel, 1996). As shown in Bischi et al., 1999b, under the assumption $\mu_1 = \mu_2 = \mu$, the fixed points of (17) can be expressed by simple analytical expressions, and a range of parameters μ, λ_1, λ_2 exist such that two of them are both stable. For example, for the set of parameters used in Fig.14a, given by $\mu = 3.5$, $\lambda_1 = 0.6$, $\lambda_2 = 0.8$, four equilibria exist, indicated by O, S, E_1 and E_2 in the figure: O and S are saddle points, whereas E_1 and E_2 are both stable, each with its own basin of attraction, say $B(E_1)$ and $B(E_2)$, represented by white and light grey respectively (the dark grey region represents the basin of infinity, i.e. the set of initial conditions which generate unbounded trajectories).

In the presence of multiple stable Nash equilibria the problem of equilibrium selection arises, and this naturally leads to the question of the delimitation of the basins of attraction. As argued in section 2, the properties of the inverses of the map become important in order to understand the structure of the basins and their qualitative changes. Indeed, the map (17) is a non-invertible map, as it can be easily deduced from the fact that given a point $q' = (q_1', q_2') \in R^2$, its rank-1 preimages $T^{-1}(\mathbf{q}')$, computed by solving

the fourth degree algebraic system (17) with respect to the quantities q_1 and q_2, may be up to four. It is easy to realize that the map (17) is a noninvertible map of $Z_0 - Z_2 - Z_4$ type, its Riemann foliation is similar to the one associated with the map (14) analyzed in section 2, see Fig. 5.

Being the map T continuously differentiable, LC_{-1} coincides with the set of points on which $\det DT = 0$, which gives

$$\left(q_1 - \frac{1}{2}\right)\left(q_2 - \frac{1}{2}\right) = \frac{(1-\lambda_1)(1-\lambda_2)}{4\lambda_1\lambda_2\mu_1\mu_2} \tag{18}$$

This equation represents an equilateral hyperbola, whose two branches are denoted by $LC_{-1}^{(a)}$ and $LC_{-1}^{(b)}$ in Fig.14. It follows that also $LC = T(LC_{-1})$ is the union of two branches, say $LC^{(a)} = T(LC_{-1}^{(a)})$ and $LC^{(b)} = T(LC_{-1}^{(b)})$. The branch $LC^{(b)}$ separates the region Z_0, whose points have no preimages, from the region Z_2, the other branch $LC^{(a)}$ separates the region Z_2 from Z_4, whose points have four distinct preimages (see Fig.14).

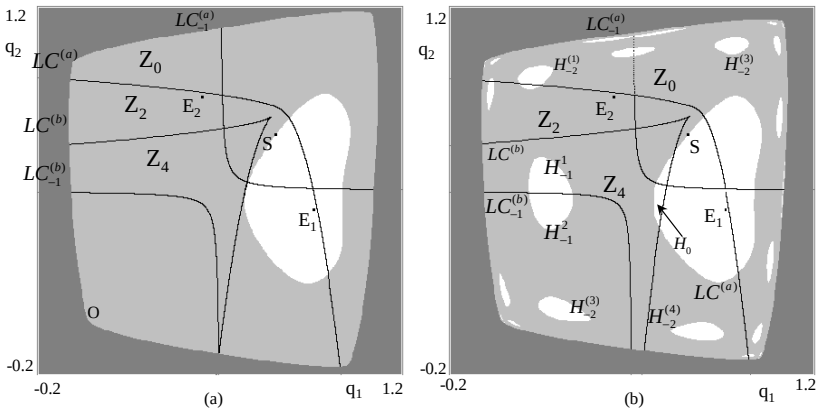

Figure 14: (a) Simply connected basin of E_1. (b) Disconnected basin of E_1 due to a contact bifurcation.

In order to understand how complex basin structures are obtained, we start from a situation in which the basins are connected sets, like the one shown in Fig 14a. In this situation, the smaller basin $B(E_1)$ is a simply connected set, and the boundary which separates the basins $B(E_1)$ and $B(E_2)$ is given by the whole stable set $W^s(S)$ of the saddle S. In Fig.14a, $W^s(S)$ is entirely included inside the regions Z_2 and Z_0. However, the fact that a

portion of $W^s(S)$ is close to $LC^{(b)}$ suggests the occurrence of a global bifurcation. If the parameters are changed, so that a contact between $W^s(S)$ and LC occurs, this contact will mark a bifurcation which causes qualitative changes in the structure of the basins. If a portion of $B(E_1)$ enters Z_4 after a contact with $LC^{(b)}$, new rank-1 preimages of that portion will appear near $LC_{-1}^{(b)}$, and such preimages must belong to $B(E_1)$. Indeed, this is the situation shown in Fig.14b, obtained after a small change of λ_1. The portion of $B(E_1)$ inside Z_4 is denoted by H_0. It has two rank-1 preimages, denoted by $H_{-1}^{(1)}$ and $H_{-1}^{(2)}$, which are located at opposite sides with respect to $LC_{-1}^{(b)}$ and merge on it (in fact, by definition, the rank-1 preimages of the arc of $LC^{(b)}$ which bound H_0 must merge along $LC_{-1}^{(b)}$). The set $H_{-1} = H_{-1}^{(1)} \cup H_{-1}^{(2)}$ constitutes a non connected portion of $B(E_1)$. Moreover, since H_{-1} belongs to the region Z_4, it has four rank-1 preimages, denoted by $H_{-2}^{(j)}$, $j = 1, ..., 4$ in Fig.14b, which constitute other four "islands" of $B(E_1)$, or "holes" of $B(E_2)$. Points of these "islands" are mapped into H_0 in two iterations of the map T. Indeed, infinitely many higher rank preimages of H_0 exist, thus giving infinitely many smaller and smaller disjoint "islands" of $B(E_1)$. Hence, at the contact between $W^s(S) = \partial B(E_1)$ and LC the basin $B(E_1)$ is transformed from a simply connected into a non connected set, constituted by infinitely many disjoint components. The larger connected component of $B(E_1)$ which contains E_1 is the immediate basin $B_0(E_1)$, and the whole basin is given by the union of the infinitely many preimages of $B_0(E_1)$: $B(E_1) = \bigcup_{n\geq 0} T^{-n}(\mathcal{B}_0(E_1)) = B_0(E_1) \cup \left[\bigcup_{n\geq 0} T^{-n}(H_0)\right]$. So, also in this two-dimensional example, the global bifurcation which causes a transformation of a basin from connected set into the union of infinitely many non connected portions, is caused by a contact between a critical set and a basin boundary. However, since the equations of the curves involved in the contact cannot be analytically expressed in terms of elementary functions, the occurrence of contact bifurcations can only be revealed numerically. This happens frequently in nonlinear dynamical systems of dimension greater than one, where the study of global bifurcations is generally obtained through an interplay between theoretical and numerical methods, and the occurrence of these bifurcations is shown by computer-assisted proofs, based on the knowledge of the properties of the critical curves and their graphical representation (see e.g. Mira et al., 1996, for many examples). This "modus operandi" is typical in the study of the global bifurcations of nonlinear two-dimensional maps.

This implies that an extension of such methods to the study of higher dimensional noninvertible maps is not easy in general. Indeed, some nontriv-

ial practical problems arise, related to the obvious reason that the computer screen is two-dimensional, so the visualization of objects in a phase spaces of dimension greater than two, and the detection of contacts among these objects as their shapes change, may become a very difficult task. In other words, the extension to higher-dimensional systems of the results on contact bifurcations, which gave so many interesting and promising results in the study of two-dimensional noninvertible maps, may become a very hard and challenging task, due to the difficulties met in the computer-assisted graphical visualization. For example, in Agiza et al., 1999, a repeated Cournot game is considered, whose time evolution is obtained by the iteration of the three-dimensional map $T : (q_1, q_2, q_3) \to (q_1', q_2', q_3')$

$$T : \begin{cases} q_1' = (1-\lambda_1)\, q_1 + \lambda_1 \mu_1 \left[q_2 \left(1 - q_2\right) + q_3 \left(1 - q_3\right) \right] \\ q_2' = (1-\lambda_2)\, q_2 + \lambda_2 \mu_2 \left[q_3 \left(1 - q_3\right) + q_1 \left(1 - q_1\right) \right] \\ q_3' = (1-\lambda_3)\, q_3 + \lambda_3 \mu_3 \left[q_1 \left(1 - q_1\right) + q_2 \left(1 - q_2\right) \right] \end{cases} \tag{19}$$

which can be seen as the extension of the game illustrated above to the case of three players. In Agiza et al., 1999, two-dimensional sections are employed in order to visualize the basins of coexisting attractors, but this method is not useful to detect the occurrence of qualitative changes in the structure of the basins and the contact bifurcations which cause such changes. The same game has been re-examined in Bischi et al., 2001c, where enhanced graphical methods have been used to modulate the opacity of the outer objects in order "to see through", in order to visualize objects which are nested inside other objects . Moreover, the critical sets, which are now two-dimensional surfaces embedded in a three-dimensional phase space, have been represented like semi-transparent veils, so that their contacts with portions of basin boundaries, also given by two-dimensional surfaces, can be detected. Some example of the kind of graphical results obtained are shown in Fig.15, which can be considered just as snapshots of animated sequences which allow interactive rotation of the three dimensional figures. In Fig.15 the basins of four coexisting stable Nash equilibria are represented by different colors, and the region outside is the outer boundary constitutes the basin of infinity. The sequence of figures shown in Fig.15 clearly show that a contact bifurcation occurs at which one of the basins is transformed from connected into a non connected set. The occurrence of this global bifurcations is caused by a contact between a basin boundary and a critical surface, after which a portion of the immediate basin enters a zone characterized by a higher number of preimages, as explained above. In the figures the critical surfaces are not shown, because a proper visualization requires the usage of

several grades of colors. The animated sequences which emphasize the contacts can the seen in the web page associated with the paper by Bischi et al., 2001c[4].

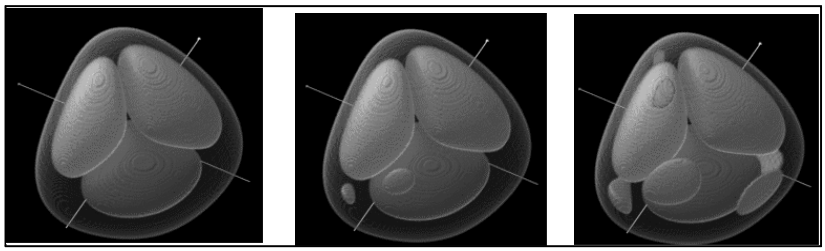

Figure 15: Example of contact bifurcation of basins of attraction in a three-dimensional map.

5 An important class of Cournot duopoly games

In this section we consider a repeated Cournot duopoly model with naive expectations, i.e. a classical discrete-time Cournot tâtonnement modeled by the iteration of the two dimensional map

$$\Phi : \begin{cases} x' = r_1(y) \\ y' = r_2(x) \end{cases} \tag{20}$$

where r_1 and r_2 are the reaction functions (or best reply functions) defined in X and Y respectively (so that Φ is defined in the rectangle $X \times Y$). In a famous paper by Rand, 1978, it is proved that quite complex dynamics, with periodic and chaotic trajectories, can emerge from the iteration of (20). Other peculiar properties of this kind of Cournot duopoly games are given in Dana and Montrucchio, 1986, where it is shown that the properties of the two-dimensional map (20) can be deduced from the properties of one-dimensional maps obtained by the composition of the reaction functions, while peculiar properties of the bifurcations associated with the two-dimensional maps (20) are given in Lupini et al., 1997. Starting from these papers, Bischi et al., 2000a, show that, in general, maps of the form (20) are characterized by multistability, i.e. coexistence of many distinct attractors,

[4]See the URL `http://bandviz.cg.tuwien.ac.at/basinviz/disjoint/`

that may be stable periodic cycles or cyclic chaotic attractors, and study the structure of their basins of attraction.

We now recall some general properties of the dynamic duopoly games (20), and we stress the peculiar structure of the critical sets and the basins.

5.1 General properties of maps Φ: $(x, y) \to (r_1(y), r_2(x))$

A trajectory of the map Φ represents the Cournot tâtonnement of a duopoly game in which the producers simultaneously update their productions at each discrete time period. Moreover, as already noticed in Dana and Montrucchio, 1986, among the possible sequences generated by the iteration of (20) there are also the so called Markov-Perfect-Equilibria (MPE henceforth) processes, where at each discrete time only one player moves, that is, the two players move alternatively, each choosing the best reply to the previous action of the other player. This occurs if the phase point (x_t, y_t) belongs alternatively to the graphs of the reaction curves $y = r_2(x)$ and $x = r_1(y)$. This condition is satisfied if the initial condition (i.c. henceforth) (x_0, y_0) belongs to a reaction curve, i.e. $y_0 = r_2(x_0)$ (player 1 moves first) or $x_0 = r_1(y_0)$ (player two moves first). This follows from the fact that the set

$$R_{12} = R_1 \cup R_2 \tag{21}$$

with $R_1 = \{(r_1(y), y) \,|y \in Y\}$ and $R_2 = \{(x, r_2(x)) \,|x \in X\}$, that represents the union of the graphs of the two reaction functions, is a trapping set for Φ, i.e. $\Phi(R_{12}) \subseteq R_{12}$. In fact, it is easy to realize that the image of a point belonging to a reaction curve belongs to the other reaction curve, so any i.c. $(x_0, y_0) \in R_{12}$ generates a trajectory entirely belonging to R_{12}, $\Phi^t(x_0, y_0) \in R_{12}\ \forall t \geq 0$. We shall call such a trajectory an MPE trajectory.

A particular MPE trajectory is a fixed point of the map Φ. In fact, (x^*, y^*) is a fixed point of Φ iff $x^* = r_1(y^*)$ and $y^* = r_2(x^*)$, i.e. a point of intersection of the graphs R_1 and R_2 of the two reaction functions,

$$(x^*, y^*) \in R_{12}\,. \tag{22}$$

While an i.c. $(x_0, y_0) \in R_{12}$ generates an MPE trajectory, a "generic" i.c. $(x_0, y_0) \notin R_{12}$ shall give rise to a Cournot tâtonnement, with (x_t, y_t) not belonging, in general, to R_{12}. Note, however, that a trajectory starting with an i.c. $(x_0, y_0) \notin R_{12}$ may enter the trapping set R_{12} after a finite number of steps, since a point of the set R_{12} can have preimages out of R_{12}.

Let us turn now to the generic dynamics. We first recall some properties of the map (20), that will be used in the following. Let

$$F(x) = r_1 \circ r_2\,(x)\ ,\ x \in X, \quad \text{and} \quad G(y) = r_2 \circ r_1\,(y)\ ,\ y \in Y \qquad (23)$$

where we assume that the sets X and Y are such that the maps F and G are well defined. Then the following three properties hold (see Dana and Montrucchio, 1986)

Property 1. $\Phi^{2k}\,(x,y) = \left(F^k(x), G^k(y)\right)$ for each integer k≥ 1.

This property easily follows from the fact that the square map Φ^2 (the second iterate of Φ) is a decoupled map, since $\Phi^2(x,y) = \Phi(r_1(y), r_2(x)) = (r_1(r_2(x)), r_2(r_1(y))) = (F(x), G(y))$.

Property 2. For each $n \geq 1$ the two one-dimensional maps F and G satisfy:

$r_1 \circ G^n(y) = r_1 \circ r_2 \circ r_1 \circ ... \circ r_2 \circ r_1(y) = F^n \circ r_1(y)$
$r_2 \circ F^n\,(x) = r_2 \circ r_1 \circ r_2 \circ ... \circ r_1 \circ r_2\,(x) = G^n \circ r_2\,(x)$

From Property 2 we deduce that the cycles of the maps F and G (and their stability properties), are strictly related. In particular, a correspondence between the cycles of the two maps is defined by the following

Property 3. If $\{x_1, ..., x_n\}$ is an n-cycle of F then $\{y_1, ..., y_n\} = \{r_2(x_1), ..., r_2(x_n)\}$ is an n-cycle of G .
If $\{y_1, ..., y_n\}$ is an n-cycle of G then $\{x_1, ..., x_n\} = \{r_1(y_1), ..., r_1(y_n)\}$ is an n-cycle of F

Such kinds of cycles of F and G shall be called conjugate. That is, for each cycle of F (resp. G), a conjugate one of G (resp. F) exists, and the two conjugate cycles have the same stability property (both are stable or both are unstable). In fact, due to the chain-rule for the derivative of composite functions, the cycle $\{x_1, ..., x_n\}$ of F and the conjugate cycle $\{y_1 = r_2(x_1), ..., y_n = r_2(x_n)\}$ of G have the same eigenvalue $\lambda = \prod_{i=1}^{n} DF(x_i) = \prod_{i=1}^{n} DG(y_i) = \prod_{i=1}^{n} Dr_1(y_i) Dr_2\,(x_i)$.

These properties show that the cycles of the Cournot map Φ are related to the cycles of the one-dimensional maps F and G defined in (23). Now we answer to the following questions: if F and G have cycles $C_F^{(p)} = \left\{x_1^*, ..., x_p^*\right\}$ and $C_G^{(q)} = \left\{y_1^*, ..., y_q^*\right\}$, of period p and q respectively, with eigenvalues $\lambda_F = \prod_{i=1}^{p} DF(x_i^*)$ and $\lambda_G = \prod_{i=1}^{q} DG(y_i^*)$ how many cycles of Φ are generated by these cycles ? and how can the points of the cycles of Φ be obtained ? and what are their stability properties ?.

We first consider the case $p = q = 1$, that is, the case of fixed points of F and G. Due to the correspondence defined by property 3, F and G have the same number of fixed points, say m, and if $X^* = \{x_1^*, ..., x_m^*\}$ is the set of fixed points of F then $Y^* = \{y_1^*, ..., y_m^*\}$, with $y_i^* = r_2(x_i^*)$, is the set of fixed points of G. Let us consider the m^2 points of the phase space of Φ obtained by the Cartesian product $X^* \times Y^*$. Among these points there are exactly m fixed points of the Cournot map Φ, belonging to $R_1 \cap R_2$, given by

$$p_i^* = (x_i^*, y_i^*) = (x_i^*, r_2(x_i^*)) \quad i = 1, ..., m \tag{24}$$

whereas the remaining $m^2 - m$ points of the form $\left(x_i^*, y_j^*\right)$, $i \neq j$, belong to 2-cycles of the map Φ. In fact

$$\begin{aligned}\Phi\left(x_i^*, y_j^*\right) &= \Phi\left(x_i^*, r_2\left(x_j^*\right)\right) = \left(r_1 \circ r_2(x_j^*), r_2\left(x_i^*\right)\right) \\ &= \left(F(x_j^*), r_2\left(x_i^*\right)\right) = \left(x_j^*, y_i^*\right)\end{aligned}$$

and, analogously,

$$\Phi\left(x_j^*, y_i^*\right) = \Phi\left(x_j^*, r_2\left(x_i^*\right)\right) = \left(x_i^*, y_j^*\right) .$$

Since each 2-cycle is formed by two points of $X^* \times Y^*$ not belonging to the trapping set R_{12} we have $N_2 = \left(m^2 - m\right)/2$ cycles of Φ of period 2, given by

$$C_\Phi^{(2)} = \left\{\left(x_i^*, r_2(x_j^*)\right), \left(x_j^*, r_2(x_i^*)\right)\right\} \;\; i < j, \; i, j = 1...m\,. \tag{25}$$

Thus the existence of m distinct fixed points of F (and consequently of G) implies the existence, for the Cournot map Φ, of
(a) m fixed points given by (24);
(b) $m(m-1)/2$ cycles of period two given by (25).

The stability of the fixed points and of the 2-cycles of Φ can be easily obtained. For the fixed points (24) we have

$$D\Phi\left(x_i^*, r_2\left(x_i^*\right)\right) = \begin{bmatrix} 0 & Dr_1\left(r_2\left(x_i^*\right)\right) \\ Dr_2\left(x_i^*\right) & 0 \end{bmatrix}$$

so the eigenvalues are $\lambda_{1,2} = \pm\sqrt{DF(x_i^*)} = \pm\sqrt{DG(y_i^*)}$, i.e. the fixed point is a stable or unstable node (focus) if the multiplier of F at the fixed point x_i^* is positive (negative) with modulus less or greater than one respectively. Note in particular that a fixed point of Φ cannot be a saddle.

For a 2-cycle, which is given by (25), we have

$$D\Phi^2\left(x_i^*, r_2\left(x_j^*\right)\right) = \begin{bmatrix} DF(x_j^*) & 0 \\ 0 & DF\left(x_i^*\right) \end{bmatrix}$$

so the eigenvalues are $\lambda_1 = DF(x_j^*)$ and $\lambda_2 = DF(x_i^*)$. Then a 2-cycle is a stable node if both the fixed points of F and G, whose coordinates give the points of the cycle, are stable, whereas it is an unstable node (saddle) if both the fixed points are unstable (one stable and one unstable). A 2-cycle of Φ cannot be a focus cycle. Note also that a 2-cycle of Φ can never be a MPE cycle, since if the points of $X^* \times Y^*$ used to form the 2-cycle belong to the trapping set R_{12} then they necessarily are fixed points of Φ. We now generalize these results to the case in which F has a cycle of odd period.

Cycles of the map Φ due to cycles of F of odd period.

Let F have a cycle of odd period $n = 2k + 1$, say $C_F^{(n)} = \{x_1^*, ..., x_n^*\}$, with eigenvalue $\lambda = \prod_{i=1}^{n} DF(x_i^*)$ (consequently G has the conjugate cycle $C_G^{(n)} = \{y_1^*, ..., y_n^*\}$ with $y_i^* = r_2\left(x_i^*\right)$, $i = 1, ..., n$, with the same eigenvalue λ). By combining the points of the Cartesian product $C_F^{(n)} \times C_G^{(n)}$ the following distinct coexisting cycles of the Cournot map Φ are obtained:

(a) one cycle of the same odd period $n = 2k + 1$ given by

$$C_\Phi^{(n)} = \left\{\Phi^t\left(x_1^*, r_2\left(x_{k+1}^*\right)\right), t = 1, ..., n\right\} \tag{26}$$

with eigenvalues $\lambda_{1,2} = \pm\sqrt{\lambda}$. Hence $C_\Phi^{(n)}$ is a stable or unstable node (or focus) depending on the modulus (and the sign) of λ.

(b) $k = (n-1)/2$ cycles of even period $2n$ given by

$$\begin{array}{l} {}^1C_\Phi^{(2n)} = \left\{\Phi^t\left(x_1^*, r_2\left(x_1^*\right)\right), t = 1, ..., 2n\right\} \\ {}^2C_\Phi^{(2n)} = \left\{\Phi^t\left(x_1^*, r_2\left(x_2^*\right)\right), t = 1, ..., 2n\right\} \\ \vdots \\ {}^kC_\Phi^{(2n)} = \left\{\Phi^t\left(x_1^*, r_2\left(x_k^*\right)\right), t = 1, ..., 2n\right\} \ . \end{array} \tag{27}$$

with eigenvalues $\lambda_1 = \lambda_2 = \lambda$ coincident with the common eigenvalue of the conjugated n-cycles of F and G, so that ${}^iC_\Phi^{(2n)}$, $i = 1, ..., k$ are stable (unstable) star nodes if the cycles $C_F^{(n)}$ and $C_G^{(n)}$ are stable (unstable)[5]. Of

[5] A star-node is a node-cycle with real eigenvalues having equal moduli (see Mira, 1987, p.194).

these $(k+1)$ cycles only ${}^1C_{\Phi}^{(2n)}$ is formed by points belonging to the trapping set R_{12}, i.e. only ${}^1C_{\Phi}^{(2n)}$ gives an MPE periodic trajectory (MPE cycle).

(c) Now let us suppose, as frequently happens, that F has more than one distinct cycles of period $n = 2k+1$, and hence the same holds for G. In this case, in addition to the points of the phase plane of Φ obtained by the Cartesian product of the pairs of conjugate cycles, there are also the points obtained by combining the points of the non-conjugate ones. For example, let F have two n-cycles $CX_F^{(n)} = \{x_1^*, ..., x_n^*\}$ and $CZ_F^{(n)} = \{z_1^*, ..., z_n^*\}$ with eigenvalues $\lambda_x = \prod_{i=1}^n DF(x_i^*)$ and $\lambda_z = \prod_{i=1}^n DF(z_i^*)$ respectively. This implies that G has the conjugate cycles $CX_G^{(n)} = \{r_2(x_1^*), ..., r_2(x_n^*)\}$ and $CZ_G^{(n)} = \{r_2(z_1^*), ..., r_2(z_n^*)\}$ with the same eigenvalues. In this case, by combining the $4n^2$ points of the Cartesian product $\left(CX_F^{(n)} \cup CZ_F^{(n)}\right) \times \left(CX_G^{(n)} \cup CZ_G^{(n)}\right)$ the $2(k+1)$ cycles listed in (26) and (27) can be obtained by using the $2n^2$ points of $\left(CX_F^{(n)} \times CZ_G^{(n)}\right) \cup \left(CZ_F^{(n)} \times CX_G^{(n)}\right)$, and by the remaining $2n^2$ points further n cycles of Φ of period $2n$ are obtained, given by

$$\begin{array}{l} {}^1M_{\Phi}^{(2n)} = \left\{\Phi^t\left(x_1^*, r_2\left(z_1^*\right)\right), t = 1, ..., 2n\right\} \\ {}^2M_{\Phi}^{(2n)} = \left\{\Phi^t\left(x_1^*, r_2\left(z_2^*\right)\right), t = 1, ..., 2n\right\} \\ \vdots \\ {}^nM_{\Phi}^{(2n)} = \left\{\Phi^t\left(x_1^*, r_2\left(z_n^*\right)\right), t = 1, ..., 2n\right\} \end{array} \tag{28}$$

The eigenvalues of the cycles (28) can be easily computed, since $D\Phi^{2n}$ is diagonal, and are given, for each cycle, by $\lambda_1 = \lambda_x$ and $\lambda_2 = \lambda_z$. We call these cycles, formed by combining the points of pairs of non-conjugate cycles of F and G, cycles of mixed type, in order to distinguish them from the cycles described in (a) and (b) (formed by combining the points of conjugate cycles of F and G), which shall be denoted as cycles of homogeneous type.

These results can be easily generalized to the case in which F has m distinct coexisting cycles of period $n = 2k+1$, say $X_{1F}^{(n)} = \{x_{11}^*, ..., x_{1n}^*\}$,..., $X_{mF}^{(n)} = \{x_{m1}^*, ..., x_{mn}^*\}$, and consequently G has the conjugate cycles $X_{1G}^{(n)} = \{r_2(x_{11}^*), ..., r_2(x_{1n}^*)\}$,..., $X_{mG}^{(n)} = \{r_2(x_{m1}^*), ..., r_2(x_{mn}^*)\}$. In this case we have:

(a) m cycles of Φ of odd period n given by

$$C_{\Phi}^{(n)} = \left\{ \Phi^t \left(x_{i_1}^*, r_2 \left(x_{i_{(k+1)}}^* \right) \right), \, t = 1, ..., n \right\}, \, i = 1, ..., m;$$

(b) mk cycles of Φ of even period $2n$, m of which are MPE cycles, of homogeneous type, i.e. made up of points belonging to the Cartesian products between pairs of conjugate cycles, according to (27);

(c) $m\,(m-1)\,n/2$ cycles of Φ of even period $2n$, of mixed type, according to (28).

Of course, if $n = 1$ (i.e. $k = 0$) these results coincide with those, already shown above, of the case of m fixed points of F.

Cycles of the map Φ due to cycles of F of even period.

Let us now consider the case in which F has a cycle of even period $n = 2k$, say $C_F^{(n)} = \{x_1^*, ..., x_n^*\}$, with eigenvalue $\lambda = \prod_{i=1}^{n} DF(x_i^*)$, and let $C_G^{(n)} = \{y_1^*, ..., y_n^*\}$, with $y_i^* = r_2(x_i^*)$, be the conjugate cycle of G, that, as usual, has the same eigenvalue. By combining the n^2 points of the Cartesian product $C_F^{(n)} \times C_G^{(n)}$, $n^2/(2n) = n/2 = k$ cycles of Φ of period $2n$, of homogeneous type, are obtained, given by

$$\begin{array}{l} {}^1C_{\Phi}^{(2n)} = \left\{ \Phi^t \left(x_1^*, r_2(x_1^*) \right), t = 1, ..., 2n \right\} \\ {}^2C_{\Phi}^{(2n)} = \left\{ \Phi^t \left(x_1^*, r_2(x_2^*) \right), t = 1, ..., 2n \right\} \\ \vdots \\ {}^kC_{\Phi}^{(2n)} = \left\{ \Phi^t \left(x_1^*, r_2(x_k^*) \right), t = 1, ..., 2n \right\} \end{array} \tag{29}$$

Of these $n/2$ cycles only ${}^1C_{\Phi}^{(2n)}$ is an MPE cycle. For each cycle ${}^iC_{\Phi}^{(2n)}$, $i = 1, ..., k$, the eigenvalues are $\lambda_1 = \lambda_2 = \lambda$. Hence all the coexisting $k = n/2$ cycles are star nodes with the same stability property as the conjugate cycles of F and G that generate them.

Also in this case cycles of mixed type can be obtained if F (and consequently G) has $m > 1$ coexisting cycles of period $n = 2k$. In fact, in addition to the m pairs of conjugated cycles, each generating k cycles of Φ of period $2n$ according to (29), the remaining $m^2 - m$ pairs of non-conjugate cycles generate $\left(m^2 - m\right) n/2$ further cycles of period $2n$ of mixed type, with eigenvalues $\lambda_1 = \prod_{i=1}^{n} F(x_i^*)$ and $\lambda_2 = \prod_{i=1}^{n} F(z_i^*)$, where x_i^* and z_i^* are points of distinct cycles of F. The periodic points of these cycles of Φ of

mixed type are given by

$$\begin{array}{l} {}^{1}M_{\Phi}^{(2n)} = \left\{\Phi^{t}\left(x_{1}^{*}, r_{2}\left(z_{1}^{*}\right)\right), t = 1, ..., 2n\right\} \\ {}^{2}M_{\Phi}^{(2n)} = \left\{\Phi^{t}\left(x_{1}^{*}, r_{2}\left(z_{2}^{*}\right)\right), t = 1, ..., 2n\right\} \\ \vdots \\ {}^{n}M_{\Phi}^{(2n)} = \left\{\Phi^{t}\left(x_{1}^{*}, r_{2}\left(z_{n}^{*}\right)\right), t = 1, ..., 2n\right\} \end{array} \tag{30}$$

and none of these is an MPE cycle. We notice that the only substantial difference between the case of cycles of F of odd period $n = 2k + 1$ and that of cycles of even period $n = 2k$ is given by the presence, in the case of odd n, of the cycle of the same odd period of Φ generated by pairs of conjugated cycles by taking the "central point" of the cycles, according to (26).

Cycles of the map Φ due to coexisting cycles of F of different periods.

Let us now consider the cycles of the Cournot map Φ obtained from the combination of points of cycles of F and G having different periods. Of course such cycles are not conjugate and will give rise to cycles of Φ of mixed type. Let $C_{F}^{(p)} = \left\{x_{1}^{*}, ..., x_{p}^{*}\right\}$ and $C_{F}^{(q)} = \left\{z_{1}^{*}, ..., z_{q}^{*}\right\}$ be a p-cycle and a q-cycle of F, with eigenvalues $\lambda_{p} = \prod_{i=1}^{p} DF(x_{i}^{*})$ and $\lambda_{q} = \prod_{i=1}^{q} DF(z_{i}^{*})$ respectively. The map G has the conjugate cycles $C_{G}^{(p)} = \left\{r_{2}(x_{1}^{*}), ..., r_{2}(x_{p}^{*})\right\}$ and $C_{G}^{(q)} = \left\{r_{2}(z_{1}^{*}), ..., r_{2}^{*}(z_{q}^{*})\right\}$ with the same eigenvalues. Let s be the least common multiple between p and q and n_{1}, n_{2} the two natural numbers such that $s = n_{1}p = n_{2}q$. Then $N = pq/s$ distinct cycles of Φ of period $2s$ are obtained by combining the pq points of $C_{F}^{(p)} \times C_{G}^{(q)} \cup C_{F}^{(q)} \times C_{G}^{(p)}$. These cycles are given by

$$\begin{array}{l} {}^{1}M_{\Phi}^{(2s)} = \left\{\Phi^{t}\left(x_{1}^{*}, r_{2}(z_{1}^{*})\right), t = 1, ..., 2s\right\} \\ {}^{2}M_{\Phi}^{(2s)} = \left\{\Phi^{t}\left(x_{1}^{*}, r_{2}(z_{2}^{*})\right), t = 1, ..., 2s\right\} \\ \vdots \\ {}^{N}M_{\Phi}^{(2s)} = \left\{\Phi^{t}\left(x_{1}^{*}, r_{2}(z_{N}^{*})\right), t = 1, ..., 2s\right\} \end{array} \tag{31}$$

All these cycles have the same eigenvalues, given by $\lambda_{1} = \lambda_{p}^{n_{1}}$ and $\lambda_{2} = \lambda_{q}^{n_{2}}$. Hence the cycles (31) are stable if and only if both the cycles $C_{F}^{(p)}$ and $C_{F}^{(q)}$ are stable. We also note that none of the cycles (31) is a MPE cycle.

From the arguments given above, the following propositions follow:

Proposition 1. Cycles of even period $2n$ of the map Φ are obtained from:

- pairs of conjugate cycles of period n, odd or even, of F and G according to (27) or (29) respectively;
- pairs of non-conjugate cycles of period n of F and G, according to (28) or (30);
- pairs of cycles of F and G of different periods p and q, such that the least common multiple between p and q is n, according to (31).

Proposition 2. Cycles of odd period $2n+1$ of the map Φ are obtained from pairs of conjugated cycles of odd period $2n+1$ of F and G according to (26).

We recall that MPE cycles can only be obtained in case (i.1) with $n > 1$ (as previously stated, MPE cycles of period 2 cannot exist). The stability properties of the cycles of the map (20) can be deduced from the stability properties of the cycles of F and G that generate them. This important feature can be expressed by the following general statement:

Proposition 3. A cycle C of the map Φ is stable if and only if the two cycles of F and G, from which the periodic points of C are obtained, are both stable.

As an example, let us consider reaction functions expressed by $r_1(y) = \mu_1 y(1-y)$ and $r_2(x) = \mu_1 x(1-x)$. In this case the functions F and G are given by the fourth degree functions

$$F(x) = r_1 \circ r_2\,(x) = \mu_1\mu_2 x\,(1-x)\left(1+\mu_2 x^2 - \mu_2 x\right) \tag{32}$$

and

$$G(y) = r_2 \circ r_1(y) = \mu_1\mu_2 y\,(1-y)\left(1+\mu_1 y^2 - \mu_1 y\right) \tag{33}$$

Let us consider the parameters $\mu_1 = 3.4$ and $\mu_2 = 3.6$, so that the function F has four fixed points: $x_0^* = 0$, $x_1^* = q^*$, $x_2^* = p^*$, $x_3^* = u^*$, all unstable. The same holds for G, whose fixed points have coordinates $y_i^* = r_2(x_i^*)$, $i = 0, ..., 3$. The Cartesian product $\{x_i^*\} \times \{y_i^*\}$ is formed by 16 points of R^2 and includes the four fixed points of the map Φ, located at the four intersections between the reaction curves (these are homogenous 1-cycles belonging to R_{12}) and six 2-cycles with periodic points out of R_{12} (i.e. not MPE cycles) three of which are on the coordinate axes.

From the properties state above, it follows that cycles of odd period of Φ can only come from cycles of the same odd period of F and G, while cycles of even period of Φ can come from several kinds of cycles of F and G, of even or odd period, with equal or different periods, conjugate or not. From Proposition 1 we can also deduce another property, which is characteristic of the Cournot maps (20):

Proposition 4. If F has a stable cycle of period $n > 2$ then the two-dimensional map Φ is characterized by multistability, i.e. it has several distinct coexisting attracting sets.

As an example let us consider again two logistic reaction functions, as given in (32) and (33). For $\mu_1 = 3.83$ and $\mu_2 = 3.84$ the map F has only one attracting cycle of period 3, say $\{x_1, x_2, x_3\}$, with eigenvalue $\lambda = 0.39$. Then from (26) and (27) we get the following coexisting attracting cycles of the map (20):

- a stable 3-cycle $\left\{\Phi^i\left(x_1, r_2(x_2)\right), i = 1, 2, 3\right\} \notin R_{12}$ (i.e. not MPE)
- a stable 6-cycle $\left\{\Phi^i\left(x_1, r_2(x_1)\right), i = 1, ..., 6\right\} \in R_{12}$ (MPE cycle)

all of homogeneous type.

The peculiar property of multistability of a Cournot map is even more evident when F has coexisting attracting cycles, because in this case also all the cycles of mixed type in (31) are attracting for Φ.

For example, consider $\mu_1 = 3.53$ and $\mu_2 = 3.55$. In this case F has a stable 2-cycle $\{x_1, x_2\}$ coexisting with a stable 4-cycle $\{z_1, ..., z_4\}$, and the same occurs for the conjugate cycles of G . Then the map Φ has five coexisting attracting cycles:

- one homogeneous cycle of period 4, with periodic points $\left\{\Phi^i\left(x_1, r_2(x_1)\right), i = 1, ..., 4\right\} \in R_{12}$, an MPE cycle (according to (29) for the 2-cycle);
- two homogeneous cycles of period 8, given by $C^1 = \left\{\Phi^i\left(z_1, r_2(z_1)\right), i = 1, ..., 8\right\} \in R_{12}$, another MPE cycle, and $C^2 = \left\{\Phi^i\left(z_1, r_2(z_2)\right), i = 1, ..., 8\right\}$ which is not MPE (according to (29) for the 4-cycle);
- two cycles of mixed type of period 8, given by $M^1 = \left\{\Phi^i\left(x_1, r_2(z_1)\right), i = 1, ..., 8\right\}$ and $M^2 = \left\{\Phi^i\left(x_1, r_2(z_2)\right), i = 1, ..., 8\right\}$, (according to (30)).

The periodic points of these cycles are represented in Fig. 16, where also their basins of attraction are shown, represented by different colors.

We close this section by noting that, due to Property 2, a cycle of G is always the image by r_2 of a cycle of F, thus we can state that the study of only one of the maps defined in (23) is sufficient to give a complete understanding of all the cycles of the two-dimensional map Φ and their stability properties.

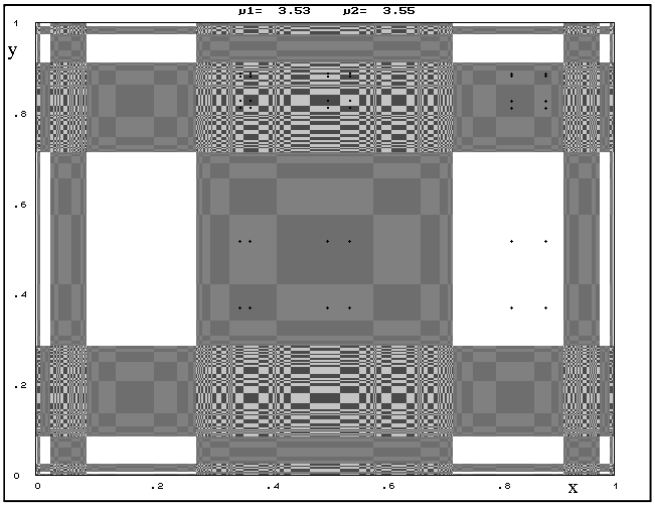

Figure 16: Basins of different coexisting attracting cycles.

5.2 Basins of attraction

As we have seen, the coexistence of attracting sets is a characteristic property of the class of maps (20), thus the structure of their basins of attraction becomes of particular interest in order to predict the asymptotic behavior of the games starting from a given i.c. (x_0, y_0). The peculiar structure of the basins of attraction, clearly visible in Fig.16, is another characteristic property of the class of maps (20), and we recall in this section the results presented in Bischi et al. 2000a.

From Propositions 1 and 2 of the previous section we know that any n-cycle C of Φ, of odd or even period n, is necessarily associated with a cycle of F and one of G, say C_x and C_y respectively. Let us denote by $B(C)$ the total basin of an attractor C. It is given by $B(C) = \bigcup_{n=0}^{\infty} \Phi^{-n}(B_{im}(C))$,

where $B_{im}(C)$ is the immediate basin of C, made up of the connected components of the basin containing C. Analogously, for the one-dimensional map F we have $B(C_x) = \bigcup_{n=0}^{\infty} F^{-n}(B_{im}(C_x))$, where $B_{im}(C_x)$ is the immediate 1-dimensional basin of C_x along the x axis. The following propositions hold (for a proof see Bischi et al. 2000):

Proposition 5. Let C be an attracting cycle of Φ associated with the cycles C_x and C_z of F, then
(i) B(C)$\subseteq [B(C_x)\cup B(C_z)] \times r_2([B(C_x) \cup B(C_z)])$
(ii) B_{im}(C)$\subseteq [B_{im}(C_x)\cup B_{im}(C_z)] \times r_2([B_{im}(C_x) \cup B_{im}(C_z)])$ and B_{im}(C) is made up of rectangles which include the points of C.

Proposition 6. Let Φ be a map of the form (20). Then:
(i) The image of a horizontal segment is a vertical segment and vice-versa.
(ii) The preimages of a horizontal segment, if any, are vertical segments and vice-versa.

Proposition 7. For any periodic point P=(x_1, y_1) of the map T of period n≥ 1, the horizontal and vertical lines $y = y_1$ and $x = x_1$, issuing from P, are trapping sets for the map T^n.

From the propositions stated above it follows that any saddle cycle of T has stable and unstable sets formed by the union of segments which are parallel to the coordinate axes.

5.3 Chaotic attractors and their basins

As stressed in the seminal paper of Rand, attractors which are more complex than periodic cycles can be easily observed in the long-run dynamics of Cournot maps (20). The transition from regular (i.e. periodic) to chaotic (i.e. aperiodic, or erratic) behavior of the Cournot tâtonnement, modeled by map (20), is marked by sequences of local bifurcations that create an increasing number of cycles, both stable and unstable. As it is well known, a chaotic regime is characterized by the presence of infinite unstable periodic points and, as remarked in Rand (1978), it is interesting to know what kind of bifurcations cause the creation of such cycles as some parameter is changed.

Since the dynamical properties of the Cournot map Φ are strictly linked to those of the one-dimensional maps F and G, these local and global bifurcations are expected to extend also to the map Φ. In fact, whenever a bifurcation occurs that creates (eliminates) cycles of the map F, and thus also of G, many cycles of the Cournot map are simultaneously created (eliminated) at the same parameter's value. Such bifurcations of the map Φ are often of

particular type, due to the presence of two eigenvalues that simultaneously cross the unit circle, in which case we say that the cycles of Φ undergo a degenerate bifurcation, whose effects are generally different from those of a generic local bifurcation. In particular, a standard fold or flip bifurcation for the one-dimensional map F (or equivalently for G), is always associated with a degenerate bifurcation of Φ of fold-type (the eigenvalues cross the unit circle with $\lambda_1 = \lambda_2 = 1$), or of flip-type ($\lambda_1 = \lambda_2 = -1$), or of saddle-type ($\lambda_1 = -1$ and $\lambda_2 = 1$).

We can extend our propositions to attractors which are more complex than point cycles. The existence of such attractors occurs when the reaction functions are non monotonic functions. In fact, if the reaction functions $r_1(y)$ and $r_2(x)$ are invertible, i.e. increasing or decreasing functions, then the dynamical behavior of the Cournot map Φ is very simple, because in this case also the maps F and G are monotone. Instead, when r_1 and/or r_2 are noninvertible maps also the functions F and G are noninvertible maps. The attractors of F can be, besides k-cycles, also k-cyclic chaotic intervals or Cantor sets (a Cantor set is an attractor in Milnor's sense (Milnor, 1985), that can occur at particular bifurcation values, as the Feigenbaum points). Let us call by A_x (resp. A_y) any one of the possible attractors of F (resp. G). Then results similar to those given in Propositions 1 and 5 still hold:

Proposition 8. Let A be an attracting set of Φ. Then attracting sets of F exist , say A_x and A_z ($A_z = A_x$ or $A_z \neq A_x$), such that

(i) $A \subseteq (A_x \cup A_z) \times (r_2(A_x \cup A_z))$

(ii) $B(A) \subseteq [B(A_x) \cup B(A_z)] \times r_2([B(A_x) \cup B(A_z)])$

(iii) $B_{im}(A) \subseteq [B_{im}(A_x) \cup B_{im}(A_z)] \times r_2([B_{im}(A_x) \cup B_{im}(A_z)])$ and $B_{im}(A)$ is made up of the rectangles which include the elements of A.

More generally, the structure related to the Cartesian products for the attracting sets of Φ holds for any invariant set of Φ, also repelling, that is:

Proposition 9. Let S be any invariant set of Φ (i.e. $\Phi(S)=S$), then there exist invariant sets of F, say S_x and S_z ($S_z = S_x$ or $S_z \neq S_x$), such that

$S \subseteq (S_x \cup S_z) \times (r_2(S_x \cup S_z))$.

As we have seen, when the attracting sets of F include something more complex then a cycle, for example a chaotic set made up of k-cyclic chaotic intervals, then also the attracting sets of Φ are more complex. However, also in this case the asymptotic sets of Φ must belong to Cartesian products of attracting sets of F and G, and such two-dimensional sets may include segments and rectangles. For example, if the map F has cyclic chaotic intervals

then, following the procedure indicated in Proposition 8, cyclic chaotic attractors of the Cournot map Φ can be obtained by the Cartesian product of the cyclic chaotic intervals of F and the conjugate ones of G, so that chaotic rectangles are obtained in the phase plane of Φ.

We again consider the particular Cournot game (20) with logistic reaction functions. Consider $\mu_1 = 2.8131$ and $\mu_2 = 3.85$. The map F has 3-cyclic chaotic intervals $\{I_1, I_2, I_3\}$ inside which the generic dynamics are aperiodic. Then $\{J_1, J_2, J_3\} = \{r_2(I_1), r_2(I_2), r_2(I_3)\}$ are the conjugate chaotic intervals of G. In this case the nine rectangles of the Cartesian product $\{I_1, I_2, I_3\} \times \{J_1, J_2, J_3\} = \{I_i \times J_j,\ i, j = 1, 2, 3\}$ include an attracting set of Φ made up of 3-cyclic rectangles (see Fig.17a) coexisting with an attracting set made up of 6-cyclic rectangles (see Fig.17b), inside which the dynamics are chaotic. The two distinct basins of attraction are shown in Fig.17c.

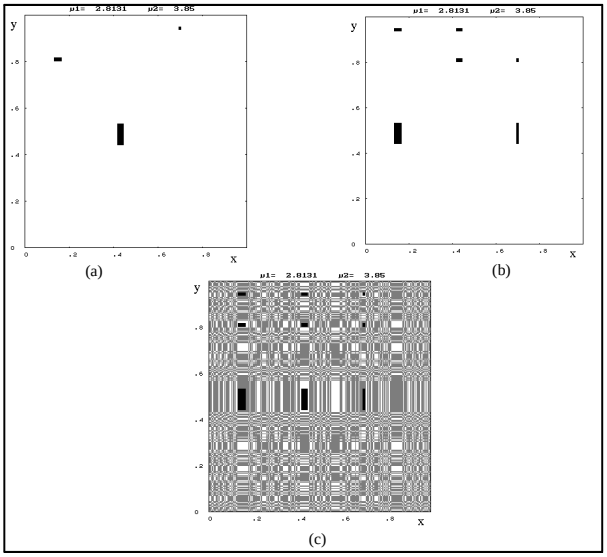

Figure 17: (a) 3-cycling chaotic rectangles. (b) 6-cycling chaotic rectangles. (c) Their basins of attraction.

As the cyclic chaotic intervals of the map F are bounded by the critical points of F, say $c^{(F)} = F\left(c_{-1}^{(F)}\right)$, and their images $c_k^{(F)} = F^k(c^{(F)})$, the sides of the chaotic rectangles of the two-dimensional map Φ are formed by

segments of lines through these critical points and parallel to the coordinate axes. Hence the boundaries of these cyclic chaotic rectangles are completely known on the basis of the knowledge of the critical points $c_k^{(F)}$ of the one dimensional map F (and those of G, given by $c_{k+1}^{(G)} = r_2\left(c_k^{(F)}\right)$).

This fact can be also seen from the more general point of view of the delimitation of the absorbing and the chaotic areas of the noninvertible maps of the plane. The critical manifold of rank-0, denoted by LC_{-1}, belongs to the locus of points at which the Jacobian determinant $|D\Phi| = Dr_2(x) \cdot Dr_1(y)$ vanishes. Hence LC_{-1} is given by the union of vertical lines and horizontal lines related to $Dr_2(x)$ and $Dr_1(y)$ respectively. Among these lines only those crossing through points of the local extrema of the reaction functions are branches of LC_{-1}. In other words, let $\overline{x}_{-1}^j$, $j = 1, ..., N$, be the points of local maxima or minima of $r_2(x)$ and $\overline{y}_{-1}^k$, $k = 1, ..., M$, be the points of local maxima or minima of $r_1(y)$, then

$$LC_{-1} = \left\{(x, y) : x = \overline{x}_{-1}^j, j = 1, ..., N\right\} \cup \\ \cup \left\{(x, y) : y = \overline{y}_{-1}^k, k = 1, ..., M\right\}. \tag{34}$$

The critical set of rank-1, denoted by LC, is obtained as $LC = \Phi(LC_{-1})$. From Proposition 6 we deduce that LC is formed by segments belonging to horizontal and vertical lines. In particular, the images by Φ of the lines $x = \overline{x}_{-1}^j$ belong to the lines of equation $y = \overline{y}^j = r_2\left(\overline{x}_{-1}^j\right)$ i.e. the horizontal lines through the maximum and minimum values of the reaction function $r_2(x)$, and the images of the lines $y = \overline{y}^k$ belong to the lines of equation $x = \overline{x}^k = r_1\left(\overline{y}_{-1}^k\right)$ which are the vertical lines through the maximum and minimum values of the reaction function $r_1(y)$.

The branches of the critical set LC separate the phase plane into regions whose points have different numbers of preimages. For example, for the Cournot map with logistic reaction curves the critical curve of rank-0 is formed by the two branches $LC_{-1} = LC_{-1}^{(a)} \cup LC_{-1}^{(b)}$, where

$$LC_{-1}^{(a)} = \left\{(x, y) \mid \ y = \frac{1}{2}\right\} \quad and \quad LC_{-1}^{(b)} = \left\{(x, y) \mid x = \frac{1}{2}\right\}. \tag{35}$$

Also LC is formed by two branches, $LC = LC^{(a)} \cup LC^{(b)}$, where $LC^{(a)} = \Phi\left(x, \frac{1}{2}\right)$ is the half-line defined by

$$x = \frac{1}{4}\mu_1, \text{ with } y \leq \frac{1}{4}\mu_2 \tag{36}$$

and $LC^{(b)} = \Phi\left(\frac{1}{2}, y\right)$ is the half-line defined by

$$y = \frac{1}{4}\mu_2 \quad \text{with} \quad x \leq \frac{1}{4}\mu_1 \tag{37}$$

In this case the two branches of LC separate a region, denoted by Z_0 in Fig.18, whose points have no real preimages, from a region, denoted by Z_4, whose points (x, y) have four real preimages, given by $x_{-1}^{(1,2)} \times y_{-1}^{(1,2)}$, where

$$x_{-1}^{(1,2)} = \frac{1}{2\mu_2}\left(\mu_2 \pm \sqrt{\mu_2^2 - 4\mu_2 y}\right) \;\; ; \;\; y_{-1}^{(1,2)} = \frac{1}{2\mu_1}\left(\mu_1 \pm \sqrt{\mu_1^2 - 4\mu_1 x}\right).$$

Critical sets of higher rank i, $i \geq 1$, defined as $LC_i = \Phi^{i+1}(LC_{-1})$ are important because generally the absorbing areas and the chaotic areas of a noninvertible map are bounded by segments of critical curves. This is true also for the absorbing and chaotic rectangles and segments of the map (20). For example in the situation shown in Fig.18 we have a chaotic attractor whose boundary is given by segments of LC, LC_1, and LC_2. As usual, segments of critical curves of higher rank bound zones inside the chaotic area where the points are more dense, i.e. are more frequently visited by the phase point of a generic trajectory.

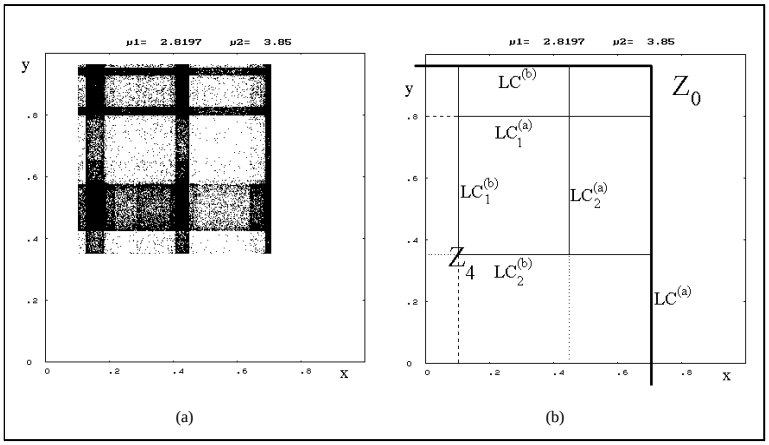

Figure 18: (a) Chaotic attractor of the Cournot map with logistic reaction curves. (b) Boundary of the chaotic attractor obtained by segments of LC_k, $k = 1, 2$.

6 Duopoly games with identical players: synchronization, riddling and intermittency phenomena

In this section we consider a dynamic duopoly game, whose time evolution is represented by the iteration of a two-dimensional map (8), in the case of identical players. This means that the dynamical system must remain the same if the variables x_1 and x_2 are interchanged, i.e. $T \circ P = P \circ T$, where $P : (x_1, x_2) \to (x_2, x_1)$ is the reflection through the diagonal

$$\Delta = \left\{(x_1, x_2) \in \mathbb{R}^2 | x_1 = x_2\right\} \ . \tag{38}$$

This symmetry property implies that the diagonal is mapped into itself, i.e., $T(\Delta) \subseteq \Delta$, which corresponds with the obvious statement that, in a deterministic framework, identical competitors, starting from identical initial conditions, behave identically for each time. The trajectories embedded into Δ, i.e. characterized by $x_1(t) = x_2(t)$ for every t, are called synchronized trajectories, and they are governed by the one-dimensional map given by the restriction of T to the invariant submanifold Δ

$$\mathbf{x}(t+1) = f(\mathbf{x}(t)) \quad \text{with} \quad f = T|_\Delta : \Delta \to \Delta. \tag{39}$$

In Bischi, Gallegati and Naimzada, 1999, the one-dimensional model (39) has been considered as the model of a representative agent whose dynamics summarize the common behavior of the two synchronized competitors.

A trajectory starting out of Δ, i.e. with $x_0 \neq y_0$, is said to synchronize if $|x_1(t) - x_2(t)| \to 0$ as $t \to +\infty$. A question which naturally arises, in the case of symmetric competition models, is whether identical competitors starting from different initial conditions will synchronize, so that the asymptotic behavior is governed by the simpler one-dimensional model (39). This question can be reformulated as follows. Let A_s be an attractor of the one-dimensional map (39). Is it also an attractor for the two-dimensional map T? Of course, an attractor A_s of the restriction f is stable with respect to perturbations along Δ, so an answer to the question raised above can be given through a study of the stability of A_s with respect to perturbations transverse to Δ (transverse stability). If A_s is a cycle, then the study of the transverse stability is the usual one, based on the modulus of the eigenvalues of the cycle in the direction transverse to Δ, whereas the problem becomes more interesting when the dynamics restricted to the invariant submanifold are chaotic. Indeed, dynamical systems with chaotic trajectories embedded into an invariant submanifold of lower dimensionality than the total phase space have

raised an increasing interest in the scientific community (see e.g. Ashwin et al., 1996, Buescu, 1997, because the phenomenon of chaos synchronization may occur (see e.g. Fujisaka and Yamada, 1983, Pecora and Carrol, 1990, Hasler and Maistrenko, 1997), i.e., the time evolution of the two competitors synchronize in the long run even if each of them behaves chaotically. Moreover, in this case, Milnor attractors (see Milnor, 1985) which are not stable in Lyapunov sense appear quite naturally in this context. To better understand the meaning of this point, we recall some definitions.

Definition. A is an asymptotically stable attractor (or topological attractor) if it is Lyapunov stable, i.e. for every neighborhood U of A there exists a neighborhood V of A such that $T^t(V) \subset U \ \forall t \geq 0$, and $B(\mathcal{A})$ contains a neighborhood of A.

In other words, If A is a topological attractor then a neighborhood $W \supset A$ exists such that $T^t(x) \to A$ as $t \to +\infty$ for any $x \in W$. In this case the stable set $B(\mathcal{A})$, also called basin of attraction, is an open set given by $B(\mathcal{A}) = \bigcup_{t \geq 0} T^{-t}(W)$.

Definition. A closed invariant set A is said to be a weak attractor in Milnor sense (or simply Milnor attractor) if its stable set $B(\mathcal{A})$ has positive Lebesgue measure.

Note that a topological attractor is also a Milnor attractor, whereas the converse is not true. Really the more general notion of Milnor attractor has been introduced to evidence the existence of invariant sets which "attract" many points even if they are not attractors in the usual topological sense.

We now recall some definitions and results related to the problem of chaos synchronization, see Buescu, 1997, for a more complete treatment. Let T be a map of the plane, Δ a one-dimensional trapping subspace and A_s a chaotic attractor (with absolutely continuous invariant measure on it) of the restriction (39) of T to Δ. The key property for the study of the transverse stability of A_s is that it includes infinitely many periodic orbits which are unstable in the direction along Δ. For any of these cycles it is easy to compute the associated eigenvalues. In fact, due to the symmetry of the map, the Jacobian matrix of T computed at any point of Δ, say $DT(x,x) = \{T_{ij}(x)\}$, is such that $T_{11} = T_{22}$ and $T_{12} = T_{21}$. The two orthogonal eigenvectors of such a symmetric matrix are one parallel to Δ, say $v_{\|} = (1,1)$, and one perpendicular to it, say $v_{\perp} = (1,-1)$, with related eigenvalues given by

$$\lambda_{\|}(x) = T_{11}(x) + T_{12}(x) \quad \text{and} \quad \lambda_{\perp}(x) = T_{11}(x) - T_{12}(x)$$

respectively. Of course, $\lambda_{\parallel}(x) = f'(x)$. Since the product of matrices with the structure of $DT(x,x)$ has the same structure as well, a k-cycle $\{s_1, ..., s_k\}$ embedded into Δ has eigenvalues $\lambda_{\parallel}^k = \prod_{i=1}^k \lambda_{\parallel}(s_i)$ and $\lambda_{\perp}^k = \prod_{i=1}^k \lambda_{\perp}(s_i)$, with eigenvectors $v_{\parallel}$ and $v_{\perp}$ respectively.

In the recent literature on chaos synchronization, stability statements are given in terms of the transverse Lyapunov exponents, by which the "average" local behavior of the trajectories in a neighborhood of the invariant set A_s can be understood, and new kinds of bifurcations can be detected , such as the riddling bifurcation or the blowout bifurcation. For a chaotic set $A_s \subset \Delta$, infinitely many transverse Lyapunov exponents can be defined as

$$\Lambda_{\perp} = \lim_{N\to\infty} \frac{1}{N} \sum_{i=0}^{N} \ln |\lambda_{\perp}(s_i)| \tag{40}$$

where $\{s_i = f^i(s_0), i \geq 0\}$ is a trajectory embedded in A_s.

If x_0 belongs to a k-cycle then $\Lambda_{\perp} = \ln |\lambda_{\perp}^k|$, so that the cycle is transversely stable if $\Lambda_{\perp} < 0$, whereas if x_0 belongs to a generic aperiodic trajectory embedded inside the chaotic set A_s then $\Lambda_{\perp}$ is the natural transverse Lyapunov exponent $\Lambda_{\perp}^{nat}$, where by the term "natural" we mean the Lyapunov exponent associated to the natural, or SBR (Sinai-Bowen-Ruelle), measure, i.e., computed for a typical trajectory taken in the chaotic attractor A_s. Since infinitely many cycles, all unstable along Δ, are embedded inside a chaotic attractor A_s, a spectrum of transverse Lyapunov exponents can be defined, see Buescu, 1997,

$$\Lambda_{\perp}^{\min} \leq ... \leq \Lambda_{\perp}^{nat} \leq ... \leq \Lambda_{\perp}^{\max} \tag{41}$$

The meaning of the inequalities in (41) can be intuitively understood on the basis of the property that $\Lambda_{\perp}^{nat}$ expresses a sort of "weighted balance" between the transversely repelling and transversely attracting cycles (see Nagai and Lai, 1997). If $\Lambda_{\perp}^{\max} < 0$, i.e. all the cycles embedded in A_s are transversely stable, then A_s is asymptotically stable, in the usual Lyapunov sense, for the two-dimensional map T. However, it may occur that some cycles embedded in the chaotic set A_s become transversely unstable, i.e. $\Lambda_{\perp}^{\max} > 0$, while $\Lambda_{\perp}^{nat} < 0$. In this case, A_s is no longer Lyapunov stable, but it continues to be a Milnor attractor, i.e. it attracts a positive (Lebesgue) measure set of points of the two-dimensional phase space. So, if $A \subset \Delta$ is a chaotic attractor of $T|_{\Delta}$ with absolutely continuous invariant measure, then a sufficient condition for a A be a Milnor, but not topological, attractor for the two-dimensional map T, is that

(a) at least one k-cycle embedded in A is transversely repelling, i.e. $\left|\lambda_{\perp}^{(k)}\right| > 1$, and

(b) the Lyapunov exponent $\Lambda_{\perp}^{nat}$ is negative.

This means that the majority of the trajectories on A are transversely attracting, but some (even infinitely many) trajectories inside A can exist whose transverse Lyapunov exponent is positive. In other words, transversely repelling trajectories can be embedded into a chaotic set which is attracting only "on average". In this case we have weak stability or stability in Milnor sense, but not asymptotic stability.

The transition from asymptotic stability to attractivity only in Milnor sense, marked by a change of sign of $\Lambda_{\perp}^{\max}$ from negative to positive, is denoted as the riddling bifurcation in Lai and Grebogi, 1996, (or bubbling bifurcation in Venkataramani et al., 1996). Even if the occurrence of such bifurcations is detected through the study of the transverse Lyapunov exponents, their effects depend on the action of the non linearities far from Δ, that is, on the global properties of the dynamical system. In fact, after the riddling bifurcation two possible scenarios can be observed according to the fate of the trajectories that are locally repelled along (or near) the local unstable manifolds of the transversely repelling cycles:

(L) they can be reinjected towards Δ, so that the dynamics of such trajectories are characterized by some bursts far from Δ before synchronizing on it (a very long sequence of such bursts, which can be observed when $\Lambda_{\perp}$ is close to zero, has been called on-off intermittency in Ott and Sommerer, 1994);

(G) they may belong to the basin of another attractor, in which case the phenomenon of riddled basins (Alexander et al., 1992) is obtained.

Some authors call local riddling the situation (L) and, by contrast, global riddling the situation (G) (see Ashwin et al. 1996, Maistrenko et al., 1997, 1998a). When also $\Lambda_{\perp}^{nat}$ becomes positive, due to the fact that the transversely unstable periodic orbits embedded into A_s have a greater weight as compared with the stable ones, a blowout bifurcation occurs, after which A_s is no longer a Milnor attractor, because it attracts a set of points of zero measure, and becomes a chaotic saddle, see Buescu, 1997. In particular, for $\lambda_{\perp}^{\min} > 0$ all the cycles embedded into Δ are transversely repelling, and A_s is called normally repelling chaotic saddle. Also the macroscopic effect of a blowout bifurcation is strongly influenced by the behavior of the dynamical system far from the invariant submanifold Δ: The trajectories starting close to the chaotic saddle may be attracted by some attracting set far from Δ

or remain inside a two-dimensional compact set located around the chaotic saddle A_s, thus giving on-off intermittency.

As noticed by many authors, (see e.g. Ashwin et al., 1996, Buescu, 1997, Hasler and Maistrenko, 1997, Maistrenko et al., 1998a,b), even if the occurrence of riddling and blowout bifurcations is detected through the transverse Lyapunov exponents, i.e. from a local analysis of the linear approximation of the map near Δ, their effects are determined by the global properties of the map. In fact, the effect of these bifurcations is related to the fate of the trajectories which are locally repelled away from a neighborhood of the Milnor attractor A_s, since they may reach another attractor or they may be folded back toward A_s by the action of the non linearities acting far from Δ. When T is a noninvertible map, as generally occurs in problems of chaos synchronization[6], the global dynamical properties can be usefully described by the method of critical curves and the reinjection of the locally repelled trajectories can be described in terms of their folding action.

This idea has been recently proposed in Bischi et al., 1998, for the study of symmetric maps arising in game theory, and in Bischi et al., 1999c, for the study of the effects of small asymmetries due to parameters mismatches. In these two papers the critical curves have been used to obtain the boundary of a compact absorbing area inside which intermittency and blowout phenomena are confined. In other words, the critical curves are used to bound a compact region of the phase plane that acts as a trapping bounded vessel inside which the trajectories starting near S are confined. In particular, in Bischi and Gardini, 1998, the concept of minimal invariant absorbing area is used in order to give a global characterization of the different dynamical scenarios related to riddling and blowout bifurcations. In order to give an example, let us consider the map (14) in the symmetric case

$$\varepsilon_1 = \varepsilon_2 = \varepsilon \quad , \qquad \mu_1 = \mu_2 = \mu \tag{42}$$

so that the map (14) becomes

$$T_s : \begin{cases} x' = \mu y(1-y) + \varepsilon(y-x) \\ y' = \mu x(1-x) + \varepsilon(x-y) \end{cases} \tag{43}$$

The restriction $T_s|_\Delta$ to the invariant diagonal Δ can be identified with the one-dimensional logistic map

$$x' = f_\mu(x) = \mu x(1-x). \tag{44}$$

[6]In fact the one-dimensional restriction f must be a noninvertible map in order to have chaotic motion along the invariant subspace Δ.

The eigenvalues of the symmetric Jacobian matrix $DT(x,x)$ are

$$\rho_{\|}(x) = \mu - 2\mu x \quad , \quad \rho_{\perp}(x) = 2\mu x - \mu - 2\varepsilon.$$

with eigenvectors which are parallel to Δ ($v_{\|} = (1,1)$) and orthogonal to Δ ($v_{\perp} = (1,-1)$) respectively. It is important to note that the coupling parameter ε only appears in the transverse eigenvalue $\lambda_{\perp}$, i.e. ε is a normal parameter: it has no influence on the dynamics along the invariant submanifold Δ, and only influences the transverse stability. This allows us to consider fixed values of the parameter μ, such that a chaotic attractor $A_s \subset \Delta$ of the map (44) exists, with an absolutely continuous invariant measure on it. So, we can study the transverse stability of A_s as the coupling between the two components, measured by the parameter ε, varies. Suitable values of the parameter μ, at which chaotic intervals for the restriction (44) exist, are obtained from the well known properties of the logistic map (see e.g. Collet and Eckmann, 1980, Mira, 1987). For example, at the parameter value $\overline{\mu}_2 = 3.5748049387592...$ the period-4 cycle of the logistic map undergoes the homoclinic bifurcation, at which four cyclic chaotic intervals are obtained by the merging of 8 cyclic chaotic intervals. By using $\overline{\mu}_2$ we get a four-band chaotic set A_s along the diagonal Δ, as shown in Fig.19a. In this case, for $\varepsilon = 0.24$ we have $\Lambda_{\perp}^{\max} > 0$ and $\Lambda_{\perp}^{nat} = -4.7 \times 10^{-3} < 0$. Hence, A_s is a Milnor attractor and local riddling occurs. The generic trajectory starting from initial conditions taken in the white region of Fig.19a leads to asymptotic synchronization. In Fig.19a the asymptotic part of a trajectory is shown, after a transient of $15,000$ iterations has been discarded. Indeed, if also the transient is represented, Fig.19b is obtained. During the transient, the time evolution of the system is characterized by several bursts away from Δ before synchronization occurs, as shown in Fig.20, where the difference $x_t - y_t$, computed along the trajectory of Fig.19, is represented versus time. It it worth to note the intermittent behavior of the trajectory: sometimes it seems to synchronize for a quite long number of iterations, then a sudden burst occurs. This phenomenon is also called on-off intermittency.

The Milnor attractor A_s is included inside a minimal invariant absorbing area whose boundary can be easily obtained by five iterations of an arc of LC_{-1}, as shown in Fig.21a. This absorbing area, obtained by the procedure outlined in section 3, constitutes a trapping region inside which the bursts observed during the transient are contained. This means that, even if it is difficult to predict the sequence of times at which asynchronous bursts occur, an estimate of their maximum amplitude can be obtained by the construction of the minimal invariant absorbing area which includes the Milnor attractor

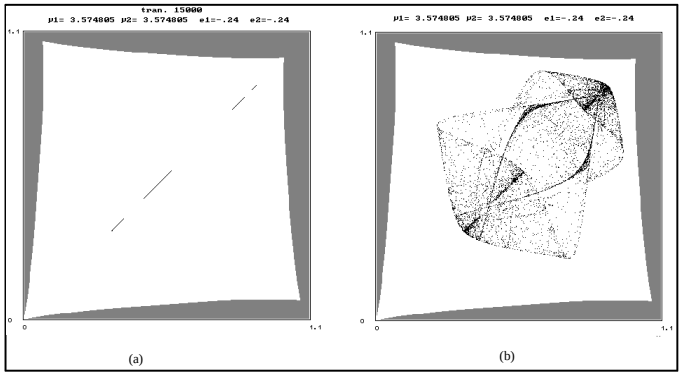

Figure 19: (a) The four-band chaotic attracting set along the diagonal. (b) The transient part of a trajectory converging to the four band chaotic set

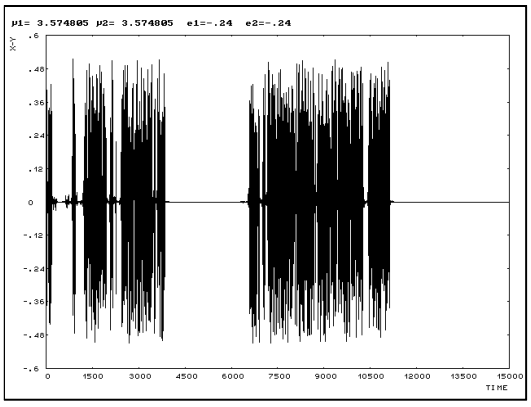

Figure 20: Bursts away from the diagonal before synchronization occurs.

on which synchronized dynamics take place. In such a situation, a method to obtain a trajectories which never synchronize, so that the bursts never stop and the iterated points fill up the whole minimal absorbing area, consists in the introduction of a small parameters' mismatch (see e.g. Bischi and Gardini, 1998), such as ε_1 slightly different from ε_2 or μ_1 slightly different from μ_2, so that the symmetry is broken. This implies that the invariance of Δ is lost, and consequently the one-dimensional Milnor attractor embedded in no longer exists. The study of the effects of small parameters' mismatches may be important in economic dynamic modelling, as stressed in Bischi et al., 1999c and Kopel et al., 2000.

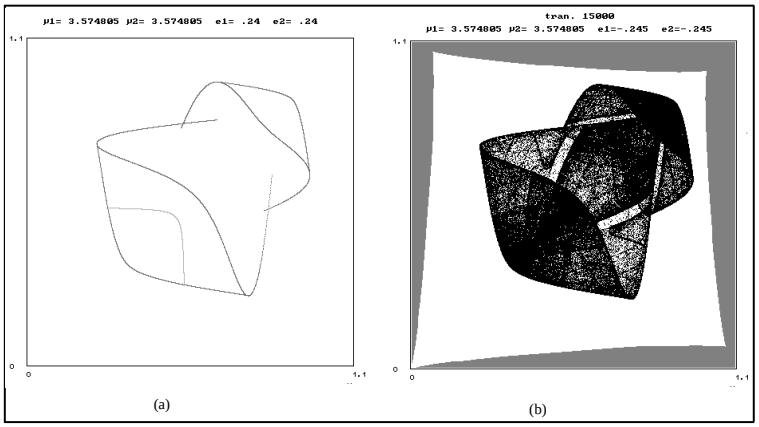

Figure 21: (a) Minimal invariant absorbing area, obtained by iteration of LC, including the Milnor attractor. (b) A trajectory filling up the absorbing area, after the introduction of a small parameters' mismatch.

A similar effect is obtained even in the symmetric case, if the value of the coupling parameter ε is increased so that $\Lambda_{\perp}^{nat}$ increases until it becomes positive, i.e. a blowout bifurcation occurs. After this bifurcation the bursts which characterize the first part of the trajectory of Fig.s 19 and 20, never stop, i.e. the firms never synchronize. A_s is now a chaotic saddle, and on-off intermittency is observed. This is what happens in the situation shown in Fig.21b, obtained for $\varepsilon = 0.245$, at which $\Lambda_{\perp}^{nat} = 2.2 \times 10^{-2} > 0$. Now the point of a generic trajectory starting from the white region fill the whole absorbing area, still bounded by segments of critical arcs.

We end this section noticing that in the case

$$\varepsilon_1 = \varepsilon_2 = 0 \tag{45}$$

we obtain the Cournot map with logistic reaction curves

$$T_{\varepsilon=0} : \begin{cases} x' = \mu_1 y(1-y) \\ y' = \mu_2 x(1-x) \end{cases} \tag{46}$$

whose properties have been analyzed in the previous section.

Acknowledgments. This work has been performed under the auspices of CNR, Italy, and under the activity of the national research project "Dynamic Models in Economics and Finance: Evolution, Uncertainty and Forecasting", MURST, Italy.

References

Abraham, R., L. Gardini and C. Mira, 1987, Chaos in discrete dynamical systems (a visual introduction in two dimension), Springer-Verlag.

Agliari, A., L. Gardini, D. Delli Gatti and M. Gallegati, 2000a, "Global dynamics in a nonlinear model for the equity ratio", Chaos, Solitons & Fractals, 11, 961-985.

Agliari, A., L. Gardini and T. Puu, 2000b, "The dynamics of a triopoly game", Chaos, Solitons & Fractals, 11, 2531-2560.

Agiza, H.N., G.I. Bischi and M. Kopel, 1999, "Multistability in a Dynamic Cournot Game with Three Oligopolists", Mathematics and Computers in Simulation, 51, 63-90.

Alexander, J.C., J.A. Yorke, Z. You and I. Kan, 1992, "Riddled basins", Int. Jou. of Bif. & Chaos, 2, 795-813

Ashwin, P., J. Buescu and I. Stewart, 1996, "From attractor to chaotic saddle: a tale of transverse instability", Nonlinearity, 9, 703-737.

Bischi, G.I. and L. Gardini, 1998, "Role of invariant and minimal absorbing areas in chaos synchronization", Physical Review E, 58, 5710-5719.

Bischi, G.I., L. Stefanini and L. Gardini, 1998 "Synchronization, intermittency and critical curves in duopoly games", Mathematics and Computers in Simulations, 44, 559-585.

Bischi, G.I., L. Gardini and C. Mira, 1999a, "Plane maps with denominator. Part I: some generic properties", International Journal of Bifurcation and Chaos, 9(1), 119-153.

Bischi, G.I., L. Gardini and M. Kopel, 1999b, "Noninvertible maps and complex basin boundaries in dynamic economic models with coexisting attractors", Proceedings SICC99, Verbania, Italy, 1999.

Bischi, G.I., M. Gallegati and A. Naimzada, 1999c, "Symmetry-Breaking bifurcations and representative firm in dynamic duopoly games", *Annals of Operations Research*, 89, 253-272.

Bischi, G.I., C. Mammana and L. Gardini, 2000a, "Multistability and cyclic attractors in duopoly games", Chaos, Solitons & Fractals, 11, pp. 543-564

Bischi, G.I., L. Gardini and M. Kopel, 2000b, "Analysis of Global Bifurcations in a Market Share Attraction Model", Journal of Economic Dynamics and Control , 24, 855-879.

Bischi, G.I. and M. Kopel, 2001, "Equilibrium Selection in a Nonlinear Duopoly Game with Adaptive Expectations", Journal of Economic Behavior and Organization, 46(1), 73-100.

Bischi, G.I., M. Kopel and A. Naimzada, 2001a, "On a rent-seeking game described by a non-invertible iterated map with denominator", Nonlinear Analysis, Theory, Methods & Applications , 47(8), 5309-5324.

Bischi, G.I., H. Dawid and M. Kopel, 2001b, "Spillover Effects and the Evolution of Firm Clusters", Journal of Economic Behavior and Organization (to appear).

Bischi, G.I., L. Mroz and H. Hauser, 2001c, "Studying basin bifurcations in nonlinear triopoly games by using 3D visualization" Nonlinear Analysis, Theory, Methods & Applications, 47(8), 5325-5341.

Buescu, J., 1997, Exotic Attractors, Birkhäuser, Boston.

Chiarella, C., R. Dieci and L. Gardini, 2001a, "Asset price dynamics in a financial market with fundamentalists and chartists " Discrete Dynamics in Nature and Society, 6, 69-99.

Chiarella, C., R. Dieci and L. Gardini, 2001b, "Speculative Behaviour and Complex Asset Price Dynamics: A Global Analysis", Journal of Economic Behavior and Organization (to appear).

Collet, P. and J.P. Eckmann, 1980, Iterated maps on the interval as dynamical systems, Birkhäuser, Boston.

Cournot, A., 1938, Recherches sur les principes matematiques de la theorie de la richesse, Hachette, Paris.

Dana, R.A. and L. Montrucchio, 1986, "Dynamic Complexity in duopoly games", Journal of Economic Theory, 40, 40-56.

Dieci, R., G.I. Bischi and L. Gardini, 2001, "From bi-stability to chaotic oscillations in a macroeconomic model", Chaos, Solitons & Fractals , 5(12),

805-822.

Fujisaka, H. and T. Yamada, 1983, "Stability theory of synchronized motion in coupled-oscillator systems", Progress of Theoretical Physics, 69 (1), 32-47.

Gardini, L., 1992, "Some global bifurcations of two-dimensional endomorphisms by use of critical lines", Nonlinear Analysis, Theory, Methods & Applications, 18, 361-399.

Grebogi, C., E. Ott and J.A. Yorke, 1983, "Crises, sudden changes in chaotic attractors and transient chaos", Physica 7D, 81-200.

Gumowski, I. and C. Mira, 1980a, $Dynamique$ Chaotique, Cepadues Editions, Toulose.

Gumowski, I. and C. Mira, 1980b, Recurrences and Discrete Dynamical Systems, Springer Verlag, Berlin.

Hasler, M. and Yu. Maistrenko, 1997, "An introduction to the synchronization of chaotic systems: coupled skew tent maps", IEEE Trans. Circuits Syst., 44 (10), 856-866.

Kopel M., 1996, "Simple and Complex Adjustment Dynamics in Cournot Duopoly Models", Chaos, Solitons & Fractals,.7(12), 2031-2048.

Kopel, M., G.I. Bischi and L. Gardini, 2000, "On new phenomena in dynamic promotional competition models with homogeneous and quasi-homogeneous firms" in Interaction and Market Structure. Essays on Heterogeneity in Economics D. Delli Gatti, M. Gallegati and A.P. Kirman (Eds.), Springer-Verlag, pp. 57-87.

Lai, Y.C.and C. Grebogi, 1996, "Noise-induced riddling in chaotic systems", Physical Review Letters 77, 5047-5050.

Lupini R., S. Lenci and L. Gardini, 1997, "Bifurcations and multistability in a class of two dimensional endomorphisms", Nonlinear Analysis T. M. & A. 28(1) 61-85.

Maistrenko, Yu., T. Kapitaniak. and P. Szuminski, 1997, "Locally and globally riddled basins in two coupled piecewise-linear maps", Physical Review E, 57 (3), 6393-6399.

Maistrenko, Yu., V.L. Maistrenko, A. Popovich and E. Mosekilde, 1998a, "Role of the Absorbing Area in Chaotic Synchronization", Physical Review Letters, 80 (8), 1638-1641.

Maistrenko, Yu., V.L. Maistrenko, A. Popovich and E. Mosekilde, 1998b, "Transverse instability and riddled basins in a system of two coupled logistic maps", Physical Review E, 57 (3), 2713-2724.

Milnor, J., 1985, "On the concept of attractor", Commun. Math Phys, 99, 177-195.

Mira, C., 1987, Chaotic Dynamics, Word Scientific, Singapore.

Mira, C., D. Fournier-Prunaret, L. Gardini, H. Kawakami and J.C. Cathala, 1994, "Basin bifurcations of two-dimensional noninvertible maps: fractalization of basins", International Journal of Bifurcation and Chaos, 4, 343-381.

Mira, C. and C. Rauzy, 1995, "Fractal aggregation of basin islands in two-dimensional quadratic noninvertible maps", International Journal of Bifurcations and Chaos, 5(4), 991-1019.

Mira, C., L. Gardini, A. Barugola and J.C. Cathala, 1996, Chaotic Dynamics in Two-Dimensional Noninvertible Maps, World Scientific, Singapore.

Nagai, Y. and Y.-C. Lai, 1997, "Periodic-orbit theory of the blowout bifurcation", Physical Review E, 56 (4), 4031-4041.

Ott, E. and J.C. Sommerer, 1994, "Blowout bifurcations: the occurrence of riddled basins and on-off intermittency", Phys. Lett. A, 188, 39-47.

Pecora, L.M. and T.L. Carrol, 1990, "Synchronization in chaotic systems", Physical Review Letters, 64 (8) pp. 821-824.

Poston T. and I. Stewart, 1978, Catastrophe Theory and its Applications, Pitman.

Puu, T., 1991, "Chaos in Duopoly Pricing", Chaos, Solitons & Fractals, 1(6), 573-581.

Puu, T., 1997, Nonlinear Economic Dynamics, Springer Verlag, Berlin.

Puu, T., 2000, Attractors, Bifurcations and Chaos, Springer Verlag, Berlin.

Rand, D., 1978, "Exotic phenomena in games and duopoly models", J. Math. Econ., 5, 173-184.

Teocharis, R.D., 1960 "On the stability of the Cournot solution on the oligopoly problem" Rev. Econ. Studies, 27, 133-134.

Van Huyck, J.B., J.P. Cook and R.C. Battalio, 1994, "Selection dynamics, asymptotic stability, and adaptive behavior", Journal of Political Economy, 102, 975-1005.

Venkataramani, S.C., B.R. Hunt and E. Ott, 1996, "Bubbling transition", Physical Review E, 54, 1346-1360.